# Ligand Affinity for Amino-Terminal and Juxtamembrane Domains of the Corticotropin Releasing Factor Type I Receptor: Regulation by G-Protein and Nonpeptide Antagonists

Sam R. J. Hoare,*,‡ Sue K. Sullivan,‡ David A. Schwarz,§ Nicholas Ling,|| Wylie W. Vale,⊥ Paul D. Crowe,‡ and Dimitri E. Grigoriadis‡

*Departments of Pharmacology, Molecular Biology, and Peptide Chemistry, Neurocrine Biosciences Inc., San Diego, California 92121-1102, and Clayton Foundation Laboratories for Peptide Biology, Salk Institute for Biological Sciences, La Jolla, California 92037*

*Received November 24, 2003; Revised Manuscript Received January 26, 2004*

ABSTRACT: Peptide ligands bind the $CRF_1$ receptor by a two-domain mechanism: the ligand's carboxyl-terminal portion binds the receptor's extracellular N-terminal domain (N-domain) and the ligand's amino-terminal portion binds the receptor's juxtamembrane domain (J-domain). Little quantitative information is available regarding this mechanism. Specifically, the microaffinity of the two interactions and their contribution to overall ligand affinity are largely undetermined. Here we measured ligand interaction with N- and J-domains expressed independently, the former (residues 1−118) fused to the activin IIB receptor's membrane-spanning α-helix ($CRF_1$-N) and the latter comprising residues 110−415 ($CRF_1$-J). We also investigated the effect of nonpeptide antagonist and G-protein on ligand affinity for N- and J-domains. Peptide agonist affinity for $CRF_1$-N was only 1.1−3.5-fold lower than affinity for the whole receptor ($CRF_1$-R), suggesting the N-domain predominantly contributes to peptide agonist affinity. Agonist interaction with $CRF_1$-J (potency for stimulating cAMP accumulation) was 12000−1500000-fold weaker than with $CRF_1$-R, indicating very weak direct agonist interaction with the J-domain. Nonpeptide antagonist affinity for $CRF_1$-J and $CRF_1$-R was indistinguishable, indicating the compounds bind predominantly the J-domain. Agonist activation of $CRF_1$-J was fully blocked by nonpeptide antagonist, suggesting antagonism results from inhibition of agonist−J-domain interaction. G-protein coupling with $CRF_1$-R (forming RG) increased peptide agonist affinity 92−1300-fold, likely resulting from enhanced agonist interaction with the J-domain rather than the N-domain. Nonpeptide antagonists, which bind the J-domain, blocked peptide agonist binding to RG, and binding of peptide antagonists, predominantly to the N-domain, was unaffected by R−G coupling. These findings extend the two-domain model quantitatively and are consistent with a simple equilibrium model of the two-domain mechanism: (1) The N-domain binds peptide agonist with moderate-to-high microaffinity, substantially increasing the local concentration of agonist and so allowing weak agonist−J-domain interaction. (2) Agonist−J-domain interaction is allosterically enhanced by receptor−G-protein interaction and inhibited by nonpeptide antagonist.

The corticotropin releasing factor 1 ($CRF_1$) receptor, a G-protein-coupled receptor (GPCR)[1] of the secretin receptor family, is activated by several related peptide ligands (*1*−*4*). The receptor is activated by CRF, a 41 amino acid peptide that is a principal physiological mediator of stress responses (*5*); by urocortin I (UCN I) (*6*), a peptide potentially involved in anxiety responses and hearing (*7*, *8*); and by the amphibian peptide sauvagine (*9*). Physiological studies have strongly implicated alteration of the CRF system in anxiety and depression (*10*), promoting the concept of $CRF_1$ receptor antagonism for treating these conditions. This hypothesis has stimulated development of high-affinity peptide and nonpeptide antagonists for the $CRF_1$ receptor (*11*, *12*).

The location of peptide ligand binding sites on the $CRF_1$ receptor has been investigated extensively. Current data are accounted for by a "two-domain" orientation, in which the C-terminal ligand portion binds the extracellular, N-terminal domain of the receptor (N-domain) and the N-terminal ligand portion binds and activates the receptor's juxtamembrane region consisting of the transmembrane domains and intervening loops (J-domain) (*11*, *13*). The N- and J-domains have both been identified as ligand binding determinants (*14*−*18*). The N-domain, expressed independently of the J-domain,

* Corresponding author. Tel: 858-658-7678. Fax: 858-658-7696. E-mail: shoare@neurocrine.com.

‡ Department of Pharmacology, Neurocrine Biosciences Inc.

§ Department of Molecular Biology, Neurocrine Biosciences Inc.

|| Department of Peptide Chemistry, Neurocrine Biosciences Inc.

⊥ Salk Institute for Biological Sciences.

[1] Abbreviations: BSA, bovine serum albumin; CRF, corticotropin-releasing factor; $CRF_1$-J, juxtamembrane $CRF_1$ receptor construct (residues 110−415); $CRF_1$-N, N-terminal $CRF_1$ receptor region (residues 1−118)/activin IIB receptor (111−494) chimeric receptor; $CRF_1$-R, full-length $CRF_1$ receptor; DPBS, Dulbecco's phosphate-buffered saline; GPCR, G-protein-coupled receptor; h, human; J-domain, juxtamembrane $CRF_1$ receptor region; m, mouse; N-domain, N-terminal $CRF_1$ receptor region; o, ovine; r, rat; R, G-protein-uncoupled receptor state; RG, G-protein-coupled receptor state; sem, standard error of the mean; UCN, urocortin.

10.1021/bi036110a CCC: $27.50 
Published on Web 03/06/2004

binds UCN I and the peptide antagonist astressin with high affinity (*15*, *16*, *18*). The J-domain is activated by a tethered N-terminal fragment of CRF (*17*). C-Terminal deamidation of CRF strongly reduces binding affinity but does not affect signaling efficacy (*5*), whereas N-terminal truncation strongly reduces signaling efficacy (*19*). Recent evidence suggests the C- and N-terminal portions of the peptide are functionally independent (*20*), suggesting functional independence of N- and J-domain binding interactions. At a higher resolution, mutagenesis and photochemical cross-linking studies have identified small amino acid sequences and amino acid residues potentially involved in peptide interaction with the N-domain (*14*, *21*−*23*) and in peptide binding and receptor activation in the J-domain (*24*−*29*).

Although molecular approaches have provided much qualitative support for the spatial orientation of the two-domain model, little quantitative information exists regarding the mechanism. Specifically, the binding energy (micro-affinity) of the two postulated interactions remains largely unknown. Measuring ligand affinity for N- and J-domains is important to more fully understand the ligand binding mechanism. While the two-domain model indicates that ligand interactions can occur, little is known about the extent of occupancy of N- and J-domains by different ligands and by different concentrations of ligand. The effect of receptor conformational change on the two-domain model also requires consideration. In common with other GPCR's, the $CRF_1$ receptor exists in multiple conformations. Specifically, the $CRF_1$ receptor is allosterically modulated by G-protein and nonpeptide antagonist (*30*−*33*). Little is known regarding how the two-domain binding mechanism is affected by these modulators.

In this study we have addressed these questions by measuring ligand interactions with the N- and J-domains expressed in isolation, comparing ligand affinity with that for the whole receptor. We investigated the extent to which different classes of ligand bind isolated N- and J-domains and the modulation of these interactions by nonpeptide antagonist and G-protein. On the basis of the findings a quantitative equilibrium model of the two-domain model is proposed for the $CRF_1$ receptor.

## MATERIALS AND METHODS

*Materials.* Peptides were synthesized by solid-phase methodology on a Beckman Coulter 990 peptide synthesizer (Fullerton, CA) using *t*-Boc-protected amino acids. The assembled peptide was deprotected with hydrogen fluoride and purified by preparative HPLC. The purity of the final product was assessed by analytical HPLC and mass spectrometric analysis using an ion-spray source. The peptides were dissolved in 10 mM acetic acid/0.1% bovine serum albumin (BSA) at a concentration of 1 mM [except UCN I (100 $\mu$M)] and stored in aliquots at −80 °C. Aliquots were used once, and any remaining solution was discarded. The following peptides were used in this study: rat/human (r/h) CRF, ovine (o) CRF, deamidated r/hCRF (r/hCRF-OH), sauvagine, hUCN I, rUCN I, mouse (m) UCN II (*34*, *35*), hUCN III (*34*, *36*), α-helical CRF [[$Met^{18}$,$Lys^{23}$,$Glu^{27,29,40}$,-$Ala^{32,41}$,$Leu^{33,36,38}$]hCRF(9−41) (*19*)], astressin [cyclo(30−33)[D-$Phe^{12}$,$Nle^{21,38}$,$Glu^{30}$,$Lys^{33}$]CRF(12−41) (*37*)], [$Tyr^0$]-astressin, $astressin_2$-B [cyclo(31−34)[D-$Phe^{11}$,$His^{12}$,CαMe-$Leu^{13,39}$,$Nle^{17}$,$Glu^{31}$,$Lys^{34}$]Ac-sauvagine(8−40) (*38*)], and antisauvagine-30 [[D-$Phe^{11}$,$His^{12}$,$Nle^{17}$]sauvagine(11−40) (*39*)]. [$^{125}$I][$Tyr^0$]Sauvagine was from PerkinElmer Life Sciences (Boston, MA) (specific activity of 2200 Ci/mmol). [$^{125}$I][$Tyr^0$]-Astressin was prepared using the chloramine T method and purified by HPLC (specific activity 2200 Ci/mol). [$^3$H]NBI 35965, custom synthesized by American Radiolabeled Chemicals (St. Louis, MO) (specific activity 25 Ci/mmol), has been used previously to specifically label the $CRF_1$ receptor (*33*). A manuscript describing the synthesis and structure of NBI 35965 and the tritiated analogue is currently being prepared for submission for publication.[2] Low-binding 96-well plates (no. 3605) were from Corning (Palo Alto, CA). G418 (geneticin), Dulbecco's phosphate-buffered saline (DPBS), and cell culture supplies were from Invitrogen (Carlsbad, CA). Fetal bovine serum was from HyClone (Logan, UT).

*Construction of Chimeric and Truncated $CRF_1$ Receptor and Expression in HEK293 Cells.* The $CRF_1$-N receptor, in pcDNA3 (Invitrogen, Carlsbad, CA), was constructed by joining the predicted N-terminal extracellular region of the rat $CRF_1$ receptor (residues 1−118) to the single membrane-spanning α-helix and intracellular region (residues 111−494) of the activin IIB receptor (*40*), as previously described (*18*). $CRF_1$-N or wild-type rat $CRF_1$ receptors in pcDNA3 were transiently expressed in HEK293T cells using Fugene 6 (Roche Molecular Biochemicals, Chicago, IL). Cells (80% confluent) in 175 $cm^2$ tissue culture flasks were washed once with DBPS and then transfected with 40 $\mu$g of plasmid and 30 $\mu$L of Fugene 6 in 8 mL of Dulbecco's modified Eagle's medium (DMEM), supplemented with 2 mM glutamine, 1 mM sodium pyruvate, and 10 mM HEPES. Cells were incubated for 3 h at 37 °C under 5% $CO_2$, and then 30 mL of DMEM supplemented with 2 mM glutamine, 1 mM sodium pyruvate, 10 mM HEPES, and 10% FBS was added per flask. Cells were cultured for an additional 2 days and then harvested for preparation of cell membranes. HEK293T cells were maintained in DMEM with 2 mM glutamine, 1 mM sodium pyruvate, 10 mM HEPES, 10% FBS, 50 IU/mL penicillin, and 50 $\mu$g/mL streptomycin.

The human $CRF_1$ receptor was amplified from a cDNA clone using the polymerase chain reaction. Oligonucleotide primers 5′-ATTGCCATGGGAGGGCACCCGCAGC-3′ and 5′-TTATCAGACTGCTGTGGACTGCTTG-3′ were modified such that the resulting PCR product incorporated a concensus Kozak translation initiation sequence and tandem stop codons in place of the native stop codon. This product was cloned into the mammalian expression vector pcDNA5/FRT/V5-His-TOPO (Invitrogen) according to the manufacturer's recommended protocol. The resulting vector was cotransfected into HEK293 Flp-In cells (Invitrogen) with the vector pOG44 encoding Flp recombinase. A stable cell line was established by selection with 50 $\mu$g/mL hygromycin.

A truncated receptor comprising the juxtamembrane domain of the $CRF_1$ receptor ($CRF_1$-J) was generated by PCR amplification of a $CRF_1$ receptor cDNA with primers 5′-AAAAAAAGCAAGGTGCACTACC-3′ and 5′-GACTGCT-GTGGACTGCTTG-3′. The amplified product incorporates the coding sequence for amino acids 110−415 of the whole receptor. This product was cloned into the vector pSecTag/

[2] Manuscript in preparation.

FRT/V5-His-TOPO, such that the resulting recombinant protein is fused to the Ig$\kappa$ leader sequence at the amino terminus and incorporates V5 and His epitope tags at the carboxyl terminus. This vector was used to establish a stable cell line in a manner similar to that described above.

The $CRF_1$-J receptor, a fragment of the human $CRF_1$ receptor, was compared with the wild-type human receptor in all cases. The $CRF_1$-N receptor, a fragment of the rat $CRF_1$ receptor, was compared with the wild-type rat receptor in all cases.

*Measurement of cAMP Accumulation.* The following were added sequentially to low-binding 96-well plates: 25 $\mu$L of buffer (DMEM without phenol red supplemented with 2 mM glutamine, 1 mM sodium pyruvate, 10 mM HEPES, 50 IU/mL penicillin, 50 $\mu$g/mL streptomycin, and 1 mM IBMX), 25 $\mu$L of ligand, and 50 $\mu$L of cell suspension (20000 cells/well). Following incubation for 30 min at 37 °C in 5% $CO_2$, cAMP was measured by chemiluminescent immunoassay (Applied Biosystems, Bedford, MA). In antagonist assays, antagonist was serially diluted in a solution of a fixed concentration of agonist.

*Preparation of Cell Membranes.* Membranes from HEK293 cells expressing $CRF_1$-J and the wild-type human $CRF_1$ receptors were prepared using a high-pressure nitrogen cell as previously described (*33*). Membranes from HEK293T cells expressing $CRF_1$-N and the wild-type rat $CRF_1$ receptors were prepared by homegenization using a tissue blender as follows: Cells in 175 $cm^2$ tissue culture flasks were washed with PBS. Cells were then dislodged by scraping in 10 mL of DPBS per plate. Cells were collected and then pelleted by centrifugation at 800*g* for 10 min at 4 °C in a Beckman GS-6R centrifuge. The cell pellet was then resuspended in assay buffer [DPBS (1.5 mM $KH_2PO_4$, 8.1 mM $Na_2HPO_4$, 2.7 mM KCl, 138 mM NaCl) supplemented with 10 mM $MgCl_2$ and 2 mM ethylene glycol bis($\beta$-aminoethyl ether)-*N*,*N*,*N*′,*N*′-tetraacetic acid, pH 7.4 with NaOH] using 6 mL of buffer per 175 $cm^2$ flask of cells. Cell lysis was then performed on ice using a Biospec Products (Bartlesville, OK) 985-370 Tissue Tearor, setting 5, two 30 s bursts 30 s apart. Isolation of cell membranes was then performed as previously described (*33*).

*Radioligand Binding Saturation Assays.* The affinity and number of radioligand binding sites were quantified using radioligand saturation experiments. The following were added sequentially to low-protein-binding 96-well plates: 25 $\mu$L of assay buffer (see Preparation of Cell Membranes, above), 50 $\mu$L of radioligand, 25 $\mu$L of buffer or unlabeled ligand in buffer, and 100 $\mu$L of cell membranes. The assay mixture was incubated for 2 h at 21 °C. Bound radioligand was then harvested by rapid filtration over GF/C filters and radioactivity determined, as previously described (*33*). The final radioligand concentration varied from approximately 3 pM to 1 nM for [$^{125}$I]astressin and from 30 pM to 10 nM for [$^3$H]NBI 35965. Nonspecific binding was measured for each concentration of radioligand, using a high concentration of the unlabeled analogue of the radioligand (320 nM for astressin, 1 $\mu$M for NBI 35965). For [$^{125}$I]astressin, the amount of HEK293 cell membrane protein added per well was 0.1, 0.15, and 1.5−2 $\mu$g for the human $CRF_1$, rat $CRF_1$, and $CRF_1$-N receptors, respectively. For [$^3$H]NBI 35965 the amount of membrane added was 4−5 $\mu$g/well for the human $CRF_1$ receptor and 25 $\mu$g/well for the $CRF_1$-J receptor. Total and nonspecific binding was measured in duplicate for each concentration of radioligand.

*Radioligand Binding Displacement Assays.* Equilibrium binding of unlabeled ligands was measured in duplicate by inhibition of radioligand binding ([$^{125}$I]astressin, [$^{125}$I]sauvagine, or [$^3$H]NBI 35965) to cell membranes. The following were added sequentially to low-binding 96-well plates: 25 $\mu$L of assay buffer, 25 $\mu$L of buffer or GTP$\gamma$S in buffer, 25 $\mu$L of radioligand, 25 $\mu$L of unlabeled ligand, and 100 $\mu$L of cell membrane suspension. The assay mixture was incubated for 2 h at 21 °C. Bound radioligand was then harvested by rapid filtration over GF/C filters and radioactivity determined, as previously described (*33*). The concentration of radioligand used was approximately 60 pM for [$^{125}$I]astressin, 90 pM for [$^{125}$I]sauvagine, and 3 nM for [$^3$H]-NBI 35965. The amount of HEK293 membrane protein used per well for [$^{125}$I]astressin displacement assays was 0.1, 0.15−0.2, and 1.5−2 $\mu$g for human $CRF_1$, rat $CRF_1$, and $CRF_1$-N receptors, respectively, with a corresponding total binding:nonspecific binding ratio of 11−15, 9−12, and 7−9, respectively. For [$^{125}$I]sauvagine the amount of membrane protein used was 2 $\mu$g/well for the human $CRF_1$ receptor, with a total binding:nonspecific binding ratio of 12−16. [$^3$H]-NBI 35965 binding displacement was measured using 3−6 $\mu$g/well for the human $CRF_1$ receptor and 25 $\mu$g/well for the $CRF_1$-J receptor, with a corresponding total binding: nonspecific binding ratio of 8−12 and 4, respectively. Nonspecific binding, as a percentage of the total radioligand added, was 1.0−3.5% for [$^{125}$I]astressin, 0.9−1.4% for [$^{125}$I]-sauvagine, and 1.2−3.7% for [$^3$H]NBI 35965. For all radioligands, total radioligand bound was less than 25% of total radioligand added.

*Data Analysis.* All curve fitting was performed using GraphPad Prism 3.00 (GraphPad Software, San Diego, CA). Ligand-stimulated cAMP accumulation was fitted to a four-parameter logistic equation. Inhibition of radioligand binding was fitted to one-affinity-state or two-affinity-state competition models, and the best fit was determined using a partial *F*-test. $K_i$ was calculated using the Cheng−Prusoff method (*41*). Radioligand saturation was analyzed using a previously described method (*33*) that takes into account depletion of free radioligand by receptor-specific and nonspecific binding of radioligand, providing an accurate measurement of $K_d$.

Statistical comparison of multiple means was performed using single-factor ANOVA, followed by post-hoc analysis using the Newman Keuls test if significant difference was determined by ANOVA. Statistical comparison of two means was performed using Student's *t*-test (two-tailed).

## RESULTS

*Expression of Isolated N- and J-Domains of the $CRF_1$ Receptor.* The strength of ligand interaction with N- and J-domains of the $CRF_1$ receptor was investigated using these domains expressed in isolation. The J-domain ($CRF_1$-J), comprising residues 110−415 of the human $CRF_1$ receptor, was expressed stably in Flp-In-HEK293 cells. The N-domain ($CRF_1$-N, residues 1−118 of the rat $CRF_1$ receptor) was fused to the single membrane-spanning α-helix of the activin IIB receptor (residues 111−494), as described previously (*18*). This chimeric receptor was expressed transiently in HEK293T cells. To initially evaluate functional expression of the

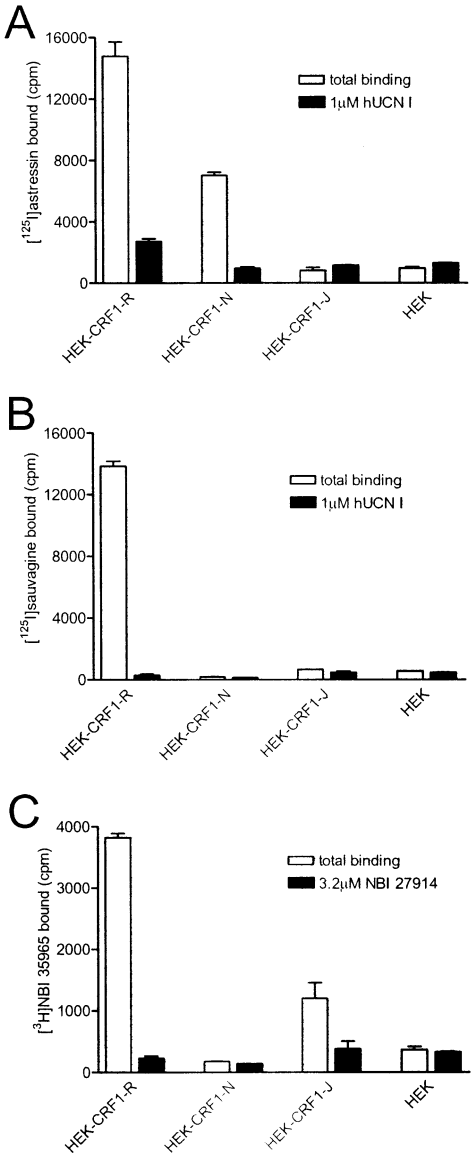


FIGURE 1: Radioligand binding to membranes from HEK293 cells expressing CRF$_1$-N, CRF$_1$-J, or wild-type receptors. Equilibrium radioligand binding was measured (Materials and Methods) using 60 pM [$^{125}$I]astressin (A), 90 pM [$^{125}$I]sauvagine (B), and 3 nM [$^3$H]NBI 35965 (C). Ligand binding was measured for cell membranes prepared from Flp-In-HEK293 cells stably expressing the wild-type human CRF$_1$ receptor (CRF$_1$-R, 5 $\mu$g of membrane protein), HEK293T cells transiently transfected with the rat CRF$_1$ N-terminal domain/activin IIB receptor chimeric receptor (CRF$_1$-N, 5 $\mu$g), Flp-In-HEK293 cells stably expressing the human CRF$_1$ receptor J-domain (CRF$_1$-J, 25 $\mu$g), and nontransfected Flp-In-HEK293 cells (HEK, 5 $\mu$g). Data are the mean $\pm$ sem of duplicates. The data are representative of two to three different experiments.

receptor fragments, we measured radioligand binding to membranes isolated from cells expressing these receptor domains or from cells expressing the whole CRF$_1$ receptor (CRF$_1$-R). The radioligands tested were the peptide antagonist [$^{125}$I]astressin, the peptide agonist [$^{125}$I]sauvagine, and the nonpeptide antagonist [$^3$H]NBI 35965. CRF$_1$-N bound [$^{125}$I]astressin (Figure 1A) but did not detectably bind [$^{125}$I]-sauvagine (Figure 1B), consistent with previous characterization of this chimeric receptor (*18*). In addition, CRF$_1$-N did not detectably bind [$^3$H]NBI 35965 (Figure 1C). CRF$_1$-J did not detectably bind the peptide ligands [$^{125}$I]astressin and [$^{125}$I]sauvagine but did bind the nonpeptide antagonist [$^3$H]-NBI 35965 (Figure 1). The human CRF$_1$-R bound all three radioligands (Figure 1), as did the rat CRF$_1$-R (data not shown), whereas no specific binding of any of the three radioligands could be detected in membranes from nontransfected cells (Figure 1).

Table 1: Radioligand Saturation of CRF$_1$-N, CRF$_1$-J, and Wild-Type (CRF$_1$-R) Receptors[a]

| receptor | radioligand | p$K_d$ ($K_d$, nM) | $B_{max}$ (pmol/mg) |
|---|---|---|---|
| rat CRF$_1$-N | [$^{125}$I]astressin | 9.66 $\pm$ 0.05[b] (0.22) | 13 $\pm$ 2 |
| human CRF$_1$-J | [$^3$H]NBI 35965 | 8.75 $\pm$ 0.06[c] (1.8) | 3.5 $\pm$ 0.3 |
| rat CRF$_1$-R | [$^{125}$I]astressin | 10.6 $\pm$ 0.1[b] (0.026) | 32 $\pm$ 1 |
| human CRF$_1$-R | [$^{125}$I]astressin | 10.2 $\pm$ 0.2 (0.065) | 62 $\pm$ 6[d] |
| human CRF$_1$-R | [$^3$H]NBI 35965 | 8.68 $\pm$ 0.02[c] (2.1) | 59 $\pm$ 3[d] |

[a] Radioligand saturation was measured (Materials and Methods) for the rat CRF$_1$-N and CRF$_1$-R receptors in HEK293T cell membranes and for the human CRF$_1$-J and CRF$_1$-R receptors expressed in Flp-In-HEK293 cells. Saturation data were fitted to one- or two-affinity-state inhibition models, and the best fit was determined using an *F*-test. A single-state model provided the best fit to the data ($p > 0.05$). The statistical significance of differences between a radioligand's saturation parameters between different receptors was determined using Student's *t*-test. [b] $p < 0.0001$. [c] $p = 0.38$. [d] $p = 0.64$. Data are the mean $\pm$ sem ($n = 3$ or 4).

We next used radioligand saturation experiments to determine the expression level of the receptors. The number of [$^{125}$I]astressin binding sites for CRF$_1$-N was 13 $\pm$ 2 pmol/mg, lower than the $B_{max}$ for the rat CRF$_1$-R (32 $\pm$ 1 pmol/mg; Table 1, Figure 2A). CRF$_1$-J bound [$^3$H]NBI 35965 with a lower $B_{max}$ than that of the human CRF$_1$-R expressed in HEK293 cells (3.5 vs 59 pmol/mg, respectively; Table 1, Figure 2B). On the human CRF$_1$-R, [$^3$H]NBI 35965 bound an equivalent number of binding sites as [$^{125}$I]astressin (62 vs 59 pmol/mg, respectively; Table 1), consistent with the hypothesis that peptide and nonpeptide antagonist bind to a common receptor population.

*Peptide Interaction with the N-Domain of the CRF$_1$ Receptor*. Previous studies have demonstrated peptide binding to the N-domain of the CRF$_1$ receptor (*15*, *16*, *18*). Here we quantitatively evaluated the contribution of the N-domain to peptide ligand affinity by comparing affinity for rat CRF$_1$-N with that for the whole rat receptor (CRF$_1$-R). Unlabeled peptides were competed against [$^{125}$I]astressin for binding to CRF$_1$-N and CRF$_1$-R. Since CRF$_1$-N cannot couple to G-protein (lacking all intracellular regions of the CRF$_1$ receptor), ligand affinity for this receptor was compared with that for the uncoupled state (R state) of CRF$_1$-R. Receptor was uncoupled from G-protein using 30 $\mu$M GTP$\gamma$S (*32*). (To maintain equivalent experimental conditions, 30 $\mu$M GTP$\gamma$S was included in the assays for CRF$_1$-N.)

A variety of peptide agonists and antagonists fully inhibited [$^{125}$I]astressin binding to CRF$_1$-N (Figure 3). Peptide affinity for CRF$_1$-N was broadly similar to affinity for the whole receptor (Figure 3, Table 2). Interestingly, the slight differences of peptide ligand affinity between CRF$_1$-N and CRF$_1$-R appeared to be dependent upon the primary structure and/or signal transduction properties of the peptides. The agonist peptides tested (CRF, sauvagine, and UCN) bound with similar or slightly lower affinity to CRF$_1$-N than to the

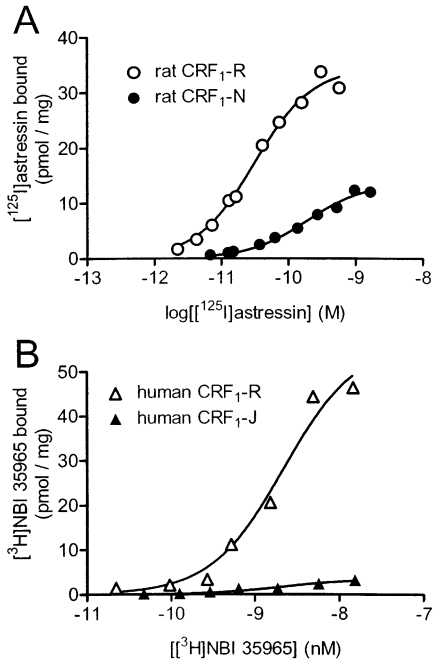


FIGURE 2: Radioligand saturation of $CRF_1$-N, $CRF_1$-J, or wild-type ($CRF_1$-R) receptors. Radioligand saturation was measured (Materials and Methods) for [$^{125}$I]astressin binding to the rat $CRF_1$-R and $CRF_1$-N receptors expressed in HEK293T cells (A) and [$^3$H]-NBI 35965 binding to the human $CRF_1$-R and $CRF_1$-J receptors expressed in Flp-In-HEK293 cells (B). Data were analyzed using single-site or two-site saturation equations, and the best fit was determined using an *F*-test. A one-site fit provided the best fit in all cases ($p > 0.05$). The data are representative of three to four different experiments.

R state of $CRF_1$-R (1.1−3.5-fold lower affinity for $CRF_1$-N; Figure 3A,C,D,I, Table 2), suggesting the N-domain contributes largely to peptide agonist affinity at the R state. The difference of affinity was greater for the N-terminally truncated antagonist peptides α-helical CRF(9−41) (Figure 3F), astressin (Figure 3G), [$^{125}$I]astressin (Figure 2A), and antisauvagine-30 (graphical data not shown); these peptides bound with 7.5−10-fold lower affinity to $CRF_1$-N compared with $CRF_1$-R (Figure 3I, Tables 1 and 2). In contrast, mUCN II (Figure 3E) and hUCN III (graphical data not shown) bound with slightly higher affinity to $CRF_1$-N than to $CRF_1$-R (2.6-fold and 1.8-fold, respectively; Figure 3I, Table 2). These two peptides are more similar in amino acid sequence to each other (45% identity) than to the remaining peptides tested (*4*).

In the two-domain model the C-terminal portion of peptide ligand is proposed to bind the N-domain of the receptor. We tested this binding orientation by measuring the effects of C-terminal ligand modification on receptor interaction, comparing the effects on $CRF_1$-N and $CRF_1$-R. The effect of C-terminal modification was evaluated by comparing CRF and deamidated CRF (CRF-OH). Deamidation of CRF eliminated detectable binding to $CRF_1$-R over the concentration range tested (up to 32 μM; compare Figure 3B with Figure 3A). The same effect was observed for $CRF_1$-N (Figure 3A,B), suggesting that the affinity-reducing effect of C-terminal deamidation is mediated, at least in part, by the N-domain of the receptor.

Peptide agonist affinity for the G-protein-uncoupled state of the $CRF_1$ receptor (R state) was surprisingly low, especially for CRF (51−95 nM) and sauvagine (140 nM)

Table 2: Comparison of Ligand Binding to $CRF_1$-N and the G-Protein-Uncoupled State of the Wild-Type ($CRF_1$-R) Receptor[a]

| ligand | p$K_i$ ($K_i$, nM) $CRF_1$-N | p$K_i$ ($K_i$, nM) $CRF_1$-R | $CRF_1$-N $K_i$/ $CRF_1$-R $K_i$ |
|---|---|---|---|
| r/hCRF | 7.25 ± 0.02 (56) | 7.29 ± 0.10 (51) | 1.1 |
| r/hCRF-OH | <4.5 (>32000) | <4.5 (>32000) | ND |
| oCRF | 6.66 ± 0.11 (220) | 7.02 ± 0.10 (95) | 2.3 |
| sauvagine | 6.31 ± 0.03 (490) | 6.86 ± 0.15[b] (140) | 3.5 |
| hUCN I | 8.43 ± 0.06 (3.7) | 8.69 ± 0.08 (2.0) | 1.9 |
| rUCN I | 8.49 ± 0.09 (3.2) | 8.88 ± 0.15 (1.3) | 2.5 |
| mUCN II | 7.24 ± 0.02 (58) | 6.81 ± 0.05 (150) | 0.39 |
| hUCN III | 6.69 ± 0.05 (200) | 6.46 ± 0.08 (350) | 0.57 |
| α-helical CRF(9−41) | 7.33 ± 0.11 (47) | 8.20 ± 0.11 (6.3) | 7.5 |
| astressin | 8.91 ± 0.07 (1.2) | 9.93 ± 0.10 (0.12) | 10 |
| astressin$_2$-B | <6 (>1000) | <6 (>1000) | ND |
| antisauvagine-30 | 6.23 ± 0.02 (590) | 7.18 ± 0.01[b] (66) | 8.9 |

[a] Ligand binding affinity was measured by displacement of [$^{125}$I]astressin binding, in the presence of 30 μM GTPγS, to the rat $CRF_1$-N or $CRF_1$-R receptors in HEK293T cell membranes (Materials and Methods). Displacement data were fitted to one- or two-affinity-state inhibition models, and the best fit was determined using an *F*-test. In all cases a single-state model provided the best fit to the data ($p > 0.05$). The log $IC_{50}$ value provided by the curve fitting analysis was converted to p$K_i$ using the Cheng−Prussoff equation, using a [$^{125}$I]astressin $K_d$ value of 0.22 nM for $CRF_1$-N and 26 pM for $CRF_1$-R (Table 1). [b] Sauvagine and antisauvagine p$K_i$ values for $CRF_1$-R are not significantly different ($p = 0.11$).

(Table 2). We have demonstrated previously that G-protein interaction with the receptor expressed in Ltk$^-$ cells and rat cerebellum considerably increases peptide agonist affinity (by as much as 890-fold) (*32*). In this previous study, ligand affinity for the receptor−G-protein complex (RG state) was measured by displacement of [$^{125}$I]sauvagine binding to the $CRF_1$ receptor. We repeated these experiments using the human $CRF_1$ receptor expressed in HEK293 cells (Table 3). All agonists, with the exception of r/hCRF-OH, bound with high affinity ($K_i$ <1 nM) to the RG state of $CRF_1$-R expressed in these cells (Table 3). The difference of peptide agonist affinity for R and RG states varied from 92-fold for hUCN I to 1300-fold for sauvagine (Table 3). Peptide antagonists astressin and antisauvagine-30 did not appreciably discriminate R and RG states (Table 3). These differences of affinity for R and RG states were similar to those measured for the receptor expressed in Ltk$^-$ cells (*32*).

In summary, the affinity of peptide agonists for $CRF_1$-N was similar to their affinity for $CRF_1$-R, suggesting the N-domain provides most of the binding energy for peptide agonists at the R state of the $CRF_1$ receptor. N-Terminally truncated peptide antagonists bound with 7.5−10-fold lower affinity to $CRF_1$-N than to $CRF_1$-R. C-Terminal deamidation eliminated detectable CRF interaction with the N-domain. G-Protein interaction with the $CRF_1$ receptor considerably increased the affinity of peptide agonists (by 92−1300-fold).

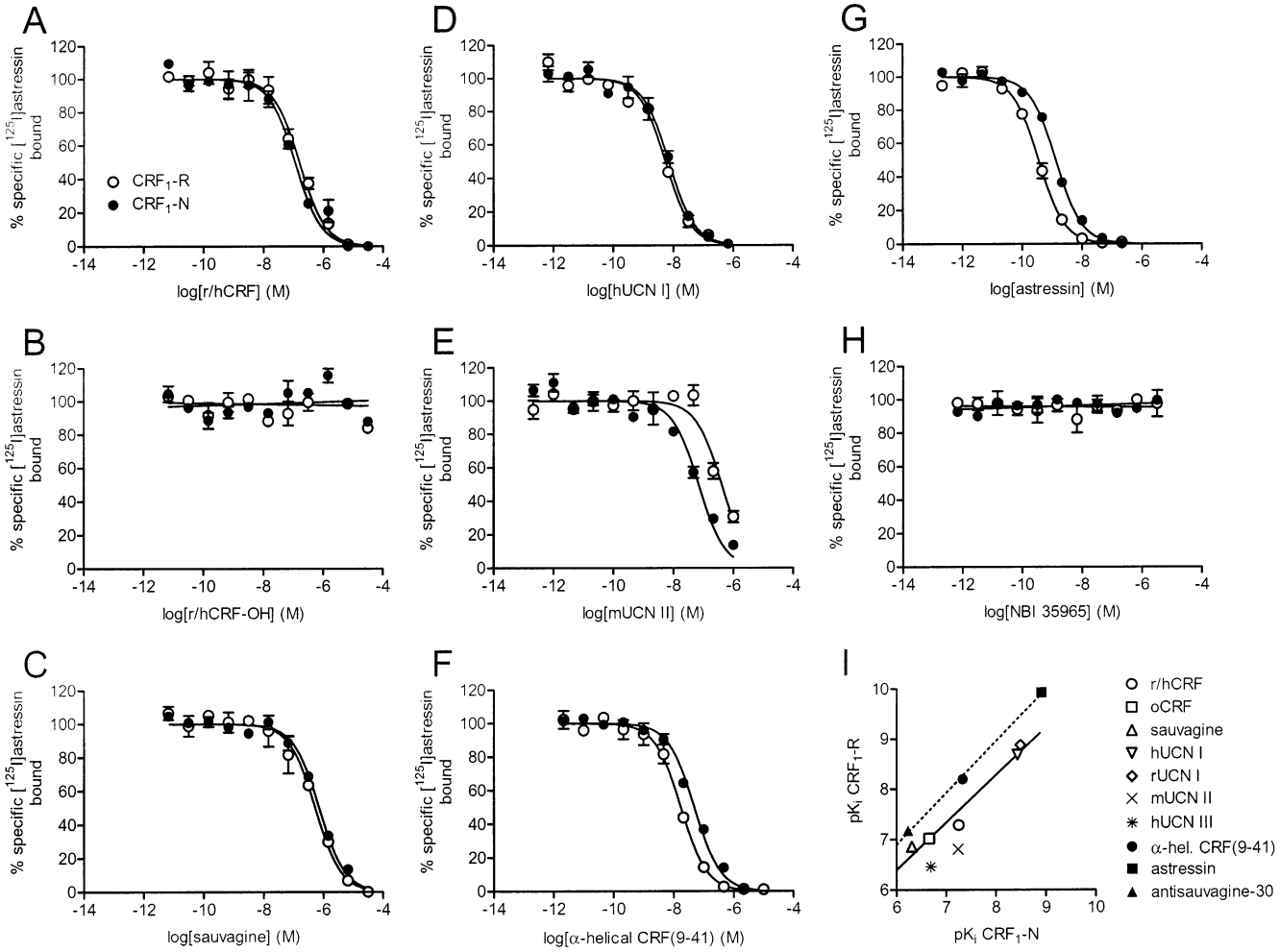


FIGURE 3: Effect of peptide and nonpeptide ligands on [$^{125}$I]astressin binding to $CRF_1$-N and wild-type ($CRF_1$-R) receptors. Displacement of [$^{125}$I]astressin binding in the presence of 30 $\mu$M GTP$\gamma$S was measured (Materials and Methods) for rat $CRF_1$-N and $CRF_1$-R receptors. Shown is the effect of r/hCRF (A), r/hCRF-OH (B), sauvagine (C), hUCN I (D), mUCN II (E), α-helical CRF(9−41) (F), astressin (G), and NBI 35965 (H). Other ligands tested were oCRF, rUCN I, hUCN III, antisauvagine-30, and astressin$_2$-B (graphical data not shown; see Table 2 for data). Data were normalized as the percentage of maximal specific [$^{125}$I]astressin binding. Data for peptide ligands were analyzed using single-site and two-site displacement equations, and the best fit was determined using an *F*-test. A one-site fit provided the best fit in all cases. The $-\log K_i$ ($pK_i$) values were compared for $CRF_1$-N and $CRF_1$-R receptors (I), and the correlation was assessed by linear regression: solid line, correlation for peptide agonists (open symbols, $r_2 = 0.965$); dashed line, correlation for peptide antagonists (closed symbols, $r_2 = 0.998$). The points are the mean ± sem of duplicates. Data are representative of three to four different experiments.

*Peptide Interaction with the J-Domain of the Receptor.* Having demonstrated successful expression of the $CRF_1$-J receptor using [$^3$H]NBI 35965 binding (Figures 1 and 2), we next evaluated the ability of peptide agonists to interact with this receptor fragment. Measurement of cAMP accumulation was used for this purpose, since radiolabeled peptide binding to $CRF_1$-J was not detectable (Figure 1). Agonist peptides CRF, CRF-OH, sauvagine, and UCN all stimulated cAMP accumulation in Flp-In-HEK293 cells expressing $CRF_1$-J (Figure 4). The $E_{max}$ of r/hCRF-OH, oCRF, and sauvagine was similar to that of r/hCRF, and hUCN I was a nearly full agonist (Table 4). The maximal stimulation of cAMP accumulation by r/hCRF was only slightly lower on $CRF_1$-J than on the human $CRF_1$-R expressed in Flp-In-HEK293 cells (8.0 vs 11 pmol of cAMP/well, respectively; Figure 4, Table 4). Therefore, the J-domain of the $CRF_1$ receptor is sufficient to support signaling by peptide agonists.

Strikingly, the potency ($pEC_{50}$) of peptide agonists for activation of $CRF_1$-J was much lower than the potency for activation of the human $CRF_1$-R (Figure 4, Table 4). This difference in potency varied between different agonists: 490-fold for r/hCRF-OH, 12000-fold for hUCN I, 200000-fold for r/hCRF, and 1500000-fold for sauvagine (Table 4). This finding suggests that direct peptide binding to the J-domain is very weak compared with peptide binding to the whole receptor. In cells expressing $CRF_1$-J, stimulation of signaling by the high concentrations of peptide required was receptor-mediated; no stimulation of cAMP accumulation was observed in nontransfected HEK293 cells (Figure 4), and high concentrations of the antagonist peptides astressin (Figure 4F) and antisauvagine-30 (data not shown) did not affect cAMP accumulation in cells expressing $CRF_1$-J (Table 4). To further test the two-domain binding orientation, the effect of C-terminal ligand modification on ligand−receptor interaction was evaluated as described above, comparing the effect of CRF with CRF-OH. Deamidation of CRF reduced the potency ($pEC_{50}$) for activation of $CRF_1$-R by 500-fold, without affecting the $E_{max}$ (compare r/hCRF with r/hCRF-OH; Figure 4A,B, Table 4). This finding, consistent with previous data (*5*), suggests that the C-terminal amide contributes to binding affinity but not to signaling efficacy.

Table 3: Displacement of [$^{125}$I]astressin and [$^{125}$I]sauvagine Binding to the Wild-Type Human $CRF_1$ Receptor in Flp-In-HEK293 Cell Membranes by Various Ligands[a]

| ligand | p$K_i$ ($K_i$, nM) vs [$^{125}$I]ast[b] + 30 $\mu$M GTP$\gamma$S | p$K_i$ ($K_i$, nM) vs [$^{125}$I]sau[c] | $K_{i([^{125}I]ast+30\ \mu M\ GTP\gamma S)}/K_{i([^{125}I]sau)}$ |
|---|---|---|---|
| r/hCRF | 6.87 ± 0.07 (130) | 9.68 ± 0.03 (0.21) | 620 |
| oCRF | 6.63 ± 0.14 (230) | 9.68 ± 0.04 (0.21) | 1100 |
| sauvagine | 6.60 ± 0.06 (250) | 9.71 ± 0.06 (0.19) | 1300 |
| hUCN I | 8.64 ± 0.01 (2.3) | 10.6 ± 0.07 (0.025) | 92 |
| rUCN I | 8.81 ± 0.12 (1.5) | 10.8 ± 0.06 (0.016) | 94 |
| astressin | 9.49 ± 0.05 (0.32) | 9.25 ± 0.01 (0.57) | 0.57 |
| antisauvagine-30 | 6.74 ± 0.04 (180) | 6.99 ± 0.01 (100) | 1.8 |

[a] Ligand binding affinity was measured by displacement of [$^{125}$I]astressin binding (in the presence of 30 $\mu$M GTP$\gamma$S) or by displacement of [$^{125}$I]sauvagine binding to the wild-type human $CRF_1$ receptor in Flp-In-HEK293 cell membranes (Materials and Methods). In the presence of GTP$\gamma$S, [$^{125}$I]astressin binds the receptor uncoupled from G-protein. [$^{125}$I]Sauvagine binds predominantly the receptor−G-protein complex, demonstrated by >90% displacement of radioligand binding produced by GTP$\gamma$S (data not shown). Displacement data were fitted to one- or two-affinity-state inhibition models, and the best fit was determined using an *F*-test. In all cases a single-state model provided the best fit to the data ($p > 0.05$). The log $IC_{50}$ value provided by the curve fitting analysis was converted to p$K_i$ using the Cheng−Prussoff equation, using a [$^{125}$I]astressin $K_d$ value of 65 pM (Table 1) and a [$^{125}$I]sauvagine $K_d$ value of 22 pM (saturation data not shown). Data are the mean ± sem ($n = 3$). [b] [$^{125}$I]ast = [$^{125}$I]astressin. [c] [$^{125}$I]sau = [$^{125}$I]sauvagine.

However, deamidation of CRF did not significantly affect the $EC_{50}$ for activation of $CRF_1$-J (Figure 4A,B, Table 4), indicating that the J-domain did not mediate the affinity-reducing effect of C-terminal deamidation of CRF.

In summary, the J-domain of the $CRF_1$ receptor was sufficient for stimulation of cAMP accumulation by peptide agonists. However, the dramatically lower potency on $CRF_1$-J compared with the wild-type receptor suggests a very low peptide affinity for the J-domain in isolation.

*Nonpeptide Antagonist Interaction with the J-Domain of the $CRF_1$ Receptor*. Numerous nonpeptide antagonists of the $CRF_1$ receptor have been developed as potential treatments for anxiety, depression, and other neuropsychiatric disorders (*11*, *12*). Previous studies have shown that the J-domain is a determinant of nonpeptide antagonist binding to the $CRF_1$ receptor (*17*, *29*). Here we quantified the contribution of the J-domain to the binding affinity of nonpeptide antagonists. In [$^3$H]NBI 35965 saturation experiments the $K_d$ for $CRF_1$-J (1.8 nM) was not significantly different from the $K_d$ for human $CRF_1$-R (2.1 nM) (Figure 2B, Table 1). Four unlabeled nonpeptide antagonists [antalarmin (*42*), NBI 27914 (*43*), NBI 35965,[2] and DMP-696 (*44*)] inhibited [$^3$H]-NBI 35965 binding to $CRF_1$-J with an affinity not significantly different from that for $CRF_1$-R (Table 5; graphical data for antalarmin and NBI 35965 shown in Figure 5A,B). These findings indicate that the J-domain contributes predominantly to the binding energy of nonpeptide antagonists. We investigated whether the N-domain contributes any detectable receptor binding energy for nonpeptide antagonists by measuring the effect of NBI 35965 on [$^{125}$I]astressin binding to $CRF_1$-N. NBI 35965 did not detectably affect [$^{125}$I]-astressin binding (Figure 3H), suggesting little or no contribution of the N-domain to nonpeptide antagonist binding. Finally, we also investigated whether peptide ligands could inhibit [$^3$H]NBI 35965 binding to $CRF_1$-J. Under the conditions of the assay it is likely the nonpeptide antagonist labels predominantly the R state (*33*). No inhibition could be detected for any peptide ligand tested (sauvagine, r/hCRF, and hUCN I, at concentrations of up to 10, 10, and 3.2 $\mu$M, respectively; data not shown). This finding is consistent with very weak direct peptide interaction with the J-domain of the R state.

The role of the J-domain in mediating functional antagonism by nonpeptide antagonists was evaluated by measuring the ability of the compounds to inhibit r/hCRF-stimulated cAMP accumulation. At the human $CRF_1$-R receptor, nonpeptide antagonists NBI 35965 and NBI 27914 fully inhibited cAMP production stimulated by 0.1 nM r/hCRF (approximately the $EC_{50}$ concentration), with an $IC_{50}$ of 41 and 110 nM, respectively (Figure 6A,B, Table 6). At the $CRF_1$-J receptor, NBI 35965 and NBI 27914 completely blocked cAMP accumulation stimulated by an $EC_{50}$ concentration (10 $\mu$M) of r/hCRF (Figure 6A,B, Table 6). This finding suggests that the J-domain contains the molecular determinants of nonpeptide antagonist binding and peptide agonist binding that enable the former to block receptor activation by the latter. The $IC_{50}$ of NBI 35965 and NBI 27914 at $CRF_1$-J was 13 and 59 nM, respectively, similar to the $IC_{50}$ on the intact receptor (Table 6).

The effect of peptide antagonists on $CRF_1$-J-mediated signaling was also investigated. As expected, the antagonists astressin and α-helical CRF(9−41) antagonized r/hCRF-stimulated cAMP accumulation via $CRF_1$-R, with an $IC_{50}$ of 2.9 and 86 nM, respectively (Figure 6C,D, Table 6). At $CRF_1$-J, high concentrations of these peptides decreased r/hCRF-stimulated cAMP accumulation (Figure 6C,D). The $IC_{50}$ for astressin at $CRF_1$-J was determined as 45 $\mu$M, 17000-fold greater than the $IC_{50}$ on the intact receptor (Table 6). These findings are consistent with a weak interaction of astressin and α-helical CRF(9−41) with the J-domain of the $CRF_1$ receptor. However, the possibility cannot be excluded that the reduction of cAMP accumulation in cells expressing $CRF_1$-J results from a nonspecific effect of the high peptide concentrations used.

## DISCUSSION

The ligand binding orientation of the $CRF_1$ receptor is well described by a two-domain model: The ligand's carboxyl-terminal portion binds the N-domain of the receptor, and the ligand's amino-terminal portion binds the J-domain of the receptor. In this study we have extended this model quantitatively by evaluating ligand microaffinity for isolated N- and J-domains. These measurements enabled us to propose an equilibrium model of the low-resolution molecular mechanism of ligand−receptor interaction (see Appendix). The principal findings are as follows: (1) The N-domain contributes almost all of the peptide ligand binding energy at the receptor uncoupled from G-protein. (2) The J-domain is sufficient for efficacious agonist-activated signaling, but with dramatically reduced agonist potency,

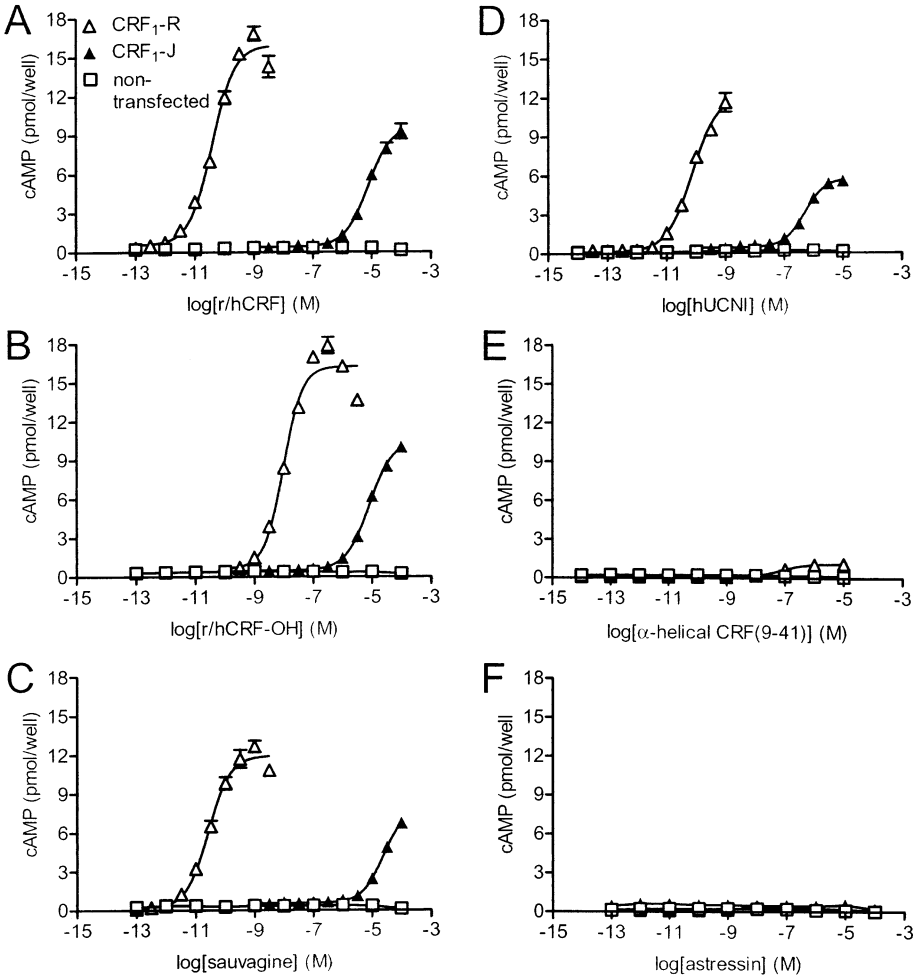


FIGURE 4: Effect of peptide ligands on cAMP accumulation in HEK293 cells expressing $CRF_1$-J and wild-type ($CRF_1$-R) receptors. Accumulation of cAMP was measured (Materials and Methods) for Flp-In-HEK293 cells expressing the human $CRF_1$-J and $CRF_1$-R receptors and for nontransfected Flp-In-HEK293 cells. Ligands tested were r/hCRF (A), r/hCRF-OH (B), sauvagine (C), hUCN I (D), α-helical CRF(9−41) (E), astressin (F), and oCRF and antisauvagine-30 (graphical data not shown; see Table 4). Data are normalized as the percentage of maximal r/hCRF-stimulated response (see legend to Table 4). The curves are fits to a four-parameter logistic equation. Data points are the mean ± sem of duplicates. Data are representative of three to four different experiments.

Table 4: Effect of CRF-Related Peptides on cAMP Accumulation via $CRF_1$-J and Wild-Type ($CRF_1$-R) Receptors[a]

| | $CRF_1$-R | | $CRF_1$-J | | |
|---|---|---|---|---|---|
| peptide | $pEC_{50}$ ($EC_{50}$, nM) | $E_{max}$/ r/hCRF $E_{max}$ (%) | $pEC_{50}$ ($EC_{50}$, nM) | $E_{max}$/ r/hCRF $E_{max}$ (%) | $EC_{50(CRF1-J)}$/ $EC_{50(CRF1-R)}$ |
| r/hCRF | 10.4 ± 0.1 (0.042) | 100 | 5.07 ± 0.03 (8400) | 100 | 200000 |
| r/hCRF-OH | 7.68 ± 0.21 (21) | 107 ± 16 | 4.99 ± 0.13 (10000) | 95 ± 8 | 490 |
| oCRF | 10.3 ± 0.1 (0.051) | 109 ± 8 | 4.95 ± 0.04 (11000) | 100 ± 5 | 220000 |
| sauvagine | 10.5 ± 0.1 (0.029) | 96 ± 7 | 4.37 ± 0.11 (42000) | 104 ± 12 | 1500000 |
| hUCN I | 10.4 ± 0.03 (0.029) | 100 ± 15 | 6.30 ± 0.04 (500) | 67 ± 7 | 12000 |
| α-helical CRF(9−41) | 7.24 ± 0.11 (58) | 12 ± 4 | ND | 0 ± 0[b] | ND |
| astressin | ND | 0 ± 0[c] | ND | −1 ± 0[c] | ND |
| antisauvagine-30 | ND | 2 ± 0[c] | ND | −1 ± 0[c] | ND |

[a] Accumulation of cAMP in Flp-In-HEK293 cells expressing the human $CRF_1$-J or $CRF_1$-R receptors was measured (Materials and Methods). Data were fitted to a four-parameter logistic equation to determine −log $EC_{50}$ ($pEC_{50}$) and $E_{max}$. The maximal net agonist-stimulated cAMP accumulation for r/hCRF was 11.0 ± 2.6 pmol/well and 8.0 ± 1.4 pmol/well for the $CRF_1$-R and $CRF_1$-J receptors, respectively, with a corresponding basal cAMP accumulation of 0.18 ± 0.13 and 0.35 ± 0.09 pmol/well, respectively ($n$ = 4). Data are the mean ± sem ($n$ =3−4). ND = not determined. [b] Response measured at 10 μM peptide. [c] Response measured at 32 μM peptide.

suggesting very weak direct agonist binding to the J-domain. (3) Nonpeptide antagonist affinity and full antagonist effect are provided predominantly if not exclusively by the J-domain. (4) As shown previously (*32*), G-protein interaction with the receptor stabilizes peptide agonist binding up to 1300-fold. The findings of this study suggest this effect is mediated by the J-domain (see below).

A number of findings in this study support or extend the two-domain model. Demonstration of ligand interactions with isolated N- and J-domains supports the model. Further support for the orientation of the model is provided by the receptor domain specificity of ligand modification effects: C-terminal CRF deamidation eliminated detectable binding to the N-domain but did not affect activation of the J-domain.

Table 5: Comparison of Nonpeptide Antagonist Affinity for Displacing [$^3$H]NBI 35965 Binding to $CRF_1$-J and Wild-Type ($CRF_1$-R) Receptors[a]

| ligand | $CRF_1$-R p$K_i$ ($K_i$, nM) | $CRF_1$-J p$K_i$ ($K_i$, nM) |
|---|---|---|
| antalarmin | 8.89 ± 0.12 (1.3) | 8.97 ± 0.10 (1.1) |
| NBI 27914 | 8.80 ± 0.03 (1.6) | 8.56 ± 0.11 (2.8) |
| NBI 35965 | 8.67 ± 0.06 (2.1) | 8.75 ± 0.13 (1.8) |
| DMP-696 | 8.72 ± 0.13 (1.9) | 8.72 ± 0.04 (1.9) |

[a] Displacement of [$^3$H]NBI 35965 binding to the human $CRF_1$-J and $CRF_1$-R receptors in Flp-In-HEK293 cell membranes was measured (Materials and Methods). Displacement data were fitted to one- or two-affinity-state inhibition models, and the best fit was determined using an *F*-test. In all cases a single-state model provided the best fit to the data ($p > 0.05$). The log $IC_{50}$ value provided by the curve fitting analysis was converted to p$K_i$ using the Cheng−Prussoff equation, using a $K_d$ value for [$^3$H]NBI 35965 of 2.1 nM for the $CRF_1$ R receptor and 1.8 nM for the $CRF_1$-J receptor (Table 1). Data are the mean ± sem ($n = 3-4$). The p$K_i$ value for the $CRF_1$-J receptor was not significantly different from the p$K_i$ value for the $CRF_1$-R receptor (*p* values of 0.28, 0.079, 0.56, and 0.99 for antalarmin, NBI 27914, NBI 35965, and DMP-696 respectively; paired two-tailed Student's *t*-test).

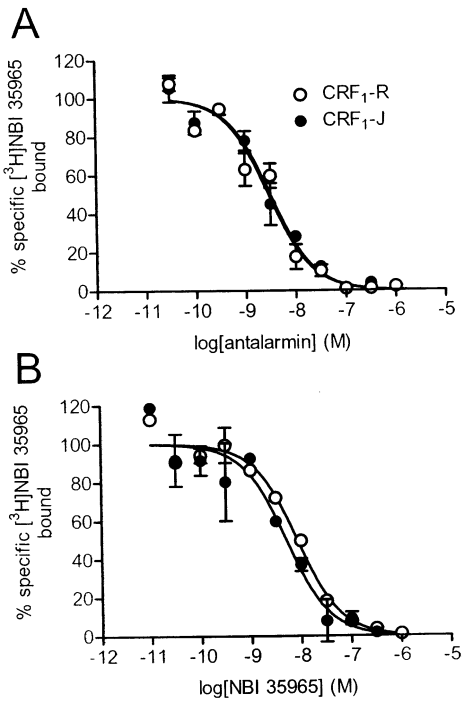


FIGURE 5: Displacement of [$^3$H]NBI 35965 binding to $CRF_1$-J and wild-type ($CRF_1$-R) receptors by unlabeled nonpeptide antagonists. Displacement of [$^3$H]NBI 35965 binding to the human $CRF_1$-J and $CRF_1$-R receptors in Flp-In-HEK293 cell membranes was measured (Materials and Methods) for nonpeptide antagonists: antalarmin (A), NBI 35965 (B), and NBI 27914 and DMP-696 (graphical data not shown; see Table 5). Data were analyzed using single-site and two-site displacement equations, and the best fit was determined using an *F*-test. A one-site fit provided the best fit in all cases. Data points are the mean ± sem of duplicates. Data are representative of three to four different experiments.

Circumstantial evidence suggests a weak interaction of astressin with the J-domain: high concentrations of astressin blocked activation of $CRF_1$-J, and astressin affinity for the whole receptor was 10-fold higher than that for $CRF_1$-N.

Our findings also address the functional independence of the two binding interactions. Previously, the N-terminal and C-terminal portions of the ligand (CRF) have been shown to be functionally independent (*20*). CRF analogues were prepared with α-helical linkers of varying lengths between the two domains. The distance between domains (4−11 amino acid residues) did not appreciably affect biological potency, whereas the relative orientation of the domains (defined by the helical register) strongly affected potency. Three of our findings suggest functional independence of the complementary domains of the receptor: (1) The N- and J-domains expressed in isolation displayed nearly full functional integrity, suggesting functional independence of receptor domains: The isolated N-domain binds peptide agonist ligands with similar affinity as the R state of the whole receptor, and the isolated J-domain mediates full high-affinity binding of nonpeptide antagonists and nearly full efficacy receptor activation by peptide agonists. [The latter finding is consistent with activation of the J-domain by a tethered N-terminal CRF fragment (*17*) and activation of a J-domain fragment of the PTH1 receptor, a related secretin receptor family GPCR (*45*).] (2) On the intact, G-protein-uncoupled receptor NBI 35965 (shown here to bind the J-domain) only weakly inhibited peptide ligand binding, and peptide ligands (shown here to bind predominantly the N-domain) only weakly inhibited [$^3$H]NBI 35965 binding (*33*). (3) A soluble N-domain protein, at concentrations up to 10 μM, did not detectably affect the cAMP level in cells expressing $CRF_1$-J.[3] Collectively, these studies of ligand and receptor suggest that the two binding interactions within the two-domain model are functionally independent.

In evaluating ligand binding properties of N- and J-domains, we were unable to demonstrate that the structure of the isolated domains is identical to the structure of these domains within the intact receptor. Alteration of receptor structure could affect ligand binding properties of the isolated fragments compared with domains within the whole receptor. However, the isolated domains displayed nearly full functional integrity (see above), implying no dramatic alteration of protein structure within the isolated domains. However, subtle structural changes might be present, so ligand affinity for $CRF_1$-N and $CRF_1$-J can only be considered approximate measurements of affinity for N- and J-domains on the whole receptor. Accurate values will require methods to measure these values directly on the whole receptor, for example, the development of peptide fragments that only bind one of the two domains [as for the PTH1 receptor (*46*, *47*)]. In addition, it is important to note that the $CRF_1$-J receptor was not optimally expressed, the expression level being about 6% of the level of the intact receptor. (In consequence, we were unable to quantify the magnitude of $CRF_1$-J's contribution to signaling efficacy, because $E_{max}$ can be affected by receptor expression.) This finding suggests that the N-domain contributes to the level of $CRF_1$ receptor expression, which might be a consequence of glycosylation; the N-domain contains the consensus sequences for N-linked glycosylation, and glycosylation is important for $CRF_1$ receptor expression (*15*, *48*).

On the basis of the strength of ligand interaction with isolated N- and J-domains we propose the first equilibrium binding model of the two-site mechanism for the $CRF_1$ receptor (Figures 7 and 8, Appendix). This model is used to estimate some of the binding parameters, to simulate occupancy of N- and J-domains by peptide ligand, and to simulate the effect of nonpeptide antagonist and G-protein

[3] R. P. Laura and S. R. J. Hoare, unpublished observations.

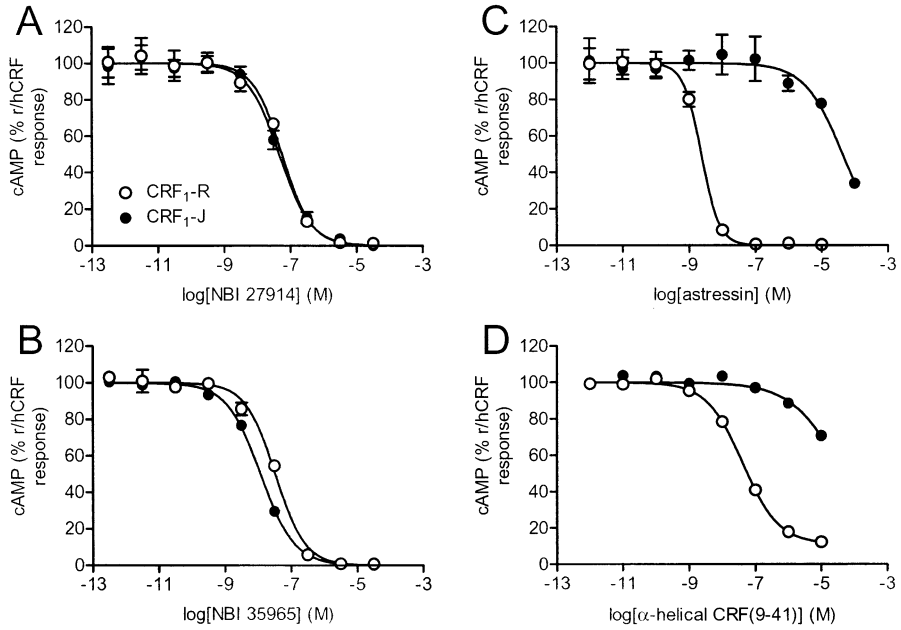


FIGURE 6: Effect of peptide and nonpeptide antagonists on r/hCRF-stimulated cAMP accumulation in HEK293 cells expressing $CRF_1$-J and wild-type ($CRF_1$-R) receptors. Antagonism of r/hCRF-stimulated cAMP accumulation was measured (Materials and Methods) for Flp-In-HEK293 cells expressing human $CRF_1$-J and $CRF_1$-R receptors. The following ligands were tested: NBI 27914 (A), NBI 35965 (B), α-helical CRF(9−41) (C), and astressin (D). Cells were added to the assay after antagonist and agonist ligands, such that the cells were exposed to both ligands simultaneously. The concentration of r/hCRF used was approximately the $EC_{50}$ for stimulation of cAMP accumulation for each receptor (10 $\mu$M for $CRF_1$-J and 0.1 nM for $CRF_1$-R; see Table 4). The curves are fits to a four-parameter logistic equation. Data points are the mean ± sem of duplicates. Data are representative of three to four different experiments.

Table 6: Antagonism of r/hCRF-Stimulated cAMP Accumulation by Peptide and Nonpeptide Antagonists on $CRF_1$-J and Wild-Type ($CRF_1$-R) Receptors[a]

| | $CRF_1$-R | | $CRF_1$-J | |
|---|---|---|---|---|
| antagonist | $pIC_{50}$ ($IC_{50}$, nM) | maximal inhibition (%) | $pIC_{50}$ ($IC_{50}$, nM) | maximal inhibition (%) |
| NBI 35965 | 7.40 ± 0.04 (41) | 101 ± 1 | 7.88 ± 0.02 (13) | 98 ± 1 |
| NBI 27914 | 6.95 ± 0.18 (110) | 98 ± 1 | 7.23 ± 0.05 (59) | 97 ± 1 |
| astressin | 8.54 ± 0.05 (2.9) | 96 ± 1 | 4.35 ± 0.02 (45000) | 100[c] |
| α-helical CRF(9−41) | 7.06 ± 0.18 (86) | 85 ± 2[b] | <5 (>10 $\mu$M) | ND |

[a] Antagonism of r/hCRF-stimulated cAMP accumulation via the human $CRF_1$-J and $CRF_1$-R receptors expressed in Flp-In-HEK293 cells was measured (Materials and Methods) using 0.1 nM r/hCRF for $CRF_1$-R and 10 $\mu$M r/hCRF for $CRF_1$-J. Net agonist-stimulated cAMP accumulation was 11.0 ± 2.6 and 8.0 ± 1.4 pmol/well for the $CRF_1$ and $CRF_1$-J receptors, respectively, with a corresponding basal cAMP accumulation (no ligand) of 0.18 ± 0.13 and 0.35 ± 0.09 pmol/well, respectively ($n$ = 4). Data were fitted to a four-parameter logistic equation to determine the −log $IC_{50}$ ($pIC_{50}$) and the maximal inhibition value, defined as $[(cAMP_{r/hCRF\ without\ antagonist} - cAMP_{lower\ plateau\ of\ inhibition\ curve})/(cAMP_{r/hCRF\ without\ antagonist} - cAMP_{no\ ligand})] \times 100$. The $cAMP_{r/hCRF\ without\ antagonist}$ value used was the upper plateau of the inhibition curve. [b] Maximal inhibition produced by α-helical CRF(9−41) on the $CRF_1$ receptor was less than 100%, by this definition, because the ligand is a partial agonist (Figure 4, Table 4). [c] The $cAMP_{lower\ plateau\ of\ inhibition\ curve}$ was fixed at the $cAMP_{no\ ligand}$ value, because the lower plateau was not approached at the highest concentration of astressin tested (100 $\mu$M). ND = not determined. Data are the mean ± sem ($n$ = 3).

on peptide ligand binding. Within this model (Scheme 1; see Appendix), ligand binds with moderate affinity to the N-domain (forming $RL_N$, defined by the equilibrium association constant $K_N$). Direct interaction with the J-domain was very weak, so ligand bound only to the J-domain ($RL_J$) likely contributes very little to the overall equilibrium occupancy of receptor. For this reason this state has been excluded, simplifying the model. However, binding of ligand to the N-domain will trap ligand within the locality of the receptor, enormously increasing the local concentration of ligand, allowing the weak interaction with the J-domain to occur (forming $RL_{NJ}$, defined by the isomerization constant $K_{NJ}$).

An approximate measurement of the microaffinity constant of the N-domain interaction ($K_N$) is provided by ligand affinity for $CRF_1$-N. The affinity for the N-domain was found to be dependent upon the class of ligand: 3.2−3.7 nM for UCN I peptides, 56−220 nM for CRF peptides, 58 nM for UCN II, 200 nM for UCN III, and 490 nM for sauvagine (Table 2). Similar differential ligand affinity for the N-domain has been reported previously for $CRF_1$ and $CRF_2$ receptors (*49*) and for the glucagon-like peptide-1 receptor (*50*). We were unable to directly measure $K_{NJ}$, but for the agonist peptides its value is likely quite low at the R state of the receptor, since ligand affinity for $CRF_1$-R was similar to that for $CRF_1$-N (implying a small contribution of the J-domain to ligand affinity; see Appendix). Occupancy of N- and J-domains was simulated under these conditions ($K_{NJ}$ = 1; Figure 7). The simulation suggests that, at the R state, an appreciable fraction of receptor occupancy is represented by ligand bound only to the N-domain ($RL_N$), with the remainder represented by ligand bitethered via N- and J-domains ($RL_{NJ}$). Surprisingly, the $CRF_1$-N $K_i$:$CRF_1$-R $K_i$ ratio was greater for peptide antagonists than peptide agonists (Table 2), suggesting a greater contribution of the J-domain to peptide antagonist affinity (at the R state). This finding suggests that antagonists and agonists differ in their inter-

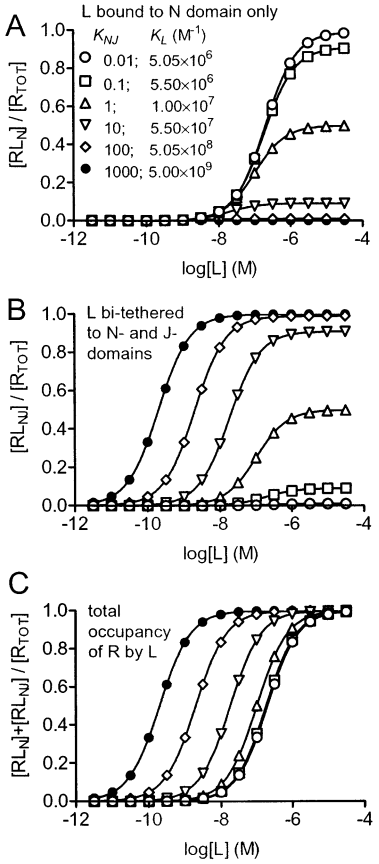


FIGURE 7: Simulation of equilibrium peptide ligand occupancy of N- and J-domains of the $CRF_1$ receptor. Scheme 1 was used to simulate peptide ligand binding to the N-domain only, $RL_N$ (A, eq 1); ligand bitethered via N- and J-domains, $RL_{NJ}$ (B, eq 2); and total ligand occupancy of the receptor, $RL_N + RL_{NJ}$ (C, eq 3). The affinity constant for peptide ligand binding to the N-domain ($K_N$) was fixed at $5 \times 10^6$ $M^{-1}$. The value of $K_{NJ}$ was varied as indicated to investigate the effect of varying strength of ligand−J-domain interaction on occupancy of the domains and the whole receptor. The resulting macroaffinity of the peptide ligand for the receptor ($K_L$) was calculated using eq 4. $[R_{TOT}]$ was set at unity so that the *y* axis represents fractional occupancy.

action with the J-domain. Finally, we found that UCN II and UCN III bound with slightly lower affinity to the whole $CRF_1$ receptor than $CRF_1$-N, suggesting that the J-domain acts as an affinity barrier to high-affinity binding of these peptides to the $CRF_1$ receptor.

We next consider the effect of G-protein on this ligand binding model. Indirect evidence suggests that G-protein interaction with the receptor enhances ligand interaction with the J-domain rather than the N-domain: (1) The J-domain contains the intracellular regions involved in binding G-protein and mediates ligand-stimulated receptor−G-protein interaction (demonstrated by efficient stimulation of cAMP production by $CRF_1$-J; Figure 4). (2) Peptide antagonists bind predominantly to the N-domain and are insensitive to receptor−G-protein interaction (Tables 2 and 3). (3) Nonpeptide antagonists, which bind the J-domain, strongly block peptide agonist binding to the RG state (*33*) and block agonist-stimulated G-protein activation (Figure 6A,B). (4) Modulation of the N-domain would require an allosteric transition though the J-domain, but the N- and J- domains are likely functionally independent to a large extent (see above). Within the framework of the model (Scheme 1; see Appendix), the enhancing effect of G-protein on agonist−J-domain interaction can be explained by an increase in the microaffinity of agonist for the J-domain, represented by an increase of $K_{NJ}$ (enhanced formation of $RL_{NJ}$ from $RL_N$). Occupancy of N- and J-domains was simulated under these conditions ($K_{NJ} = 1000$; Figure 7). In this simulation peptide agonist occupancy of the RG state was represented almost exclusively by ligand bitethered via both N- and J-domains ($RL_{NJ}$).

We next considered the effect of nonpeptide antagonist on peptide ligand binding. It is likely that nonpeptide antagonist binds the J-domain and inhibits peptide agonist binding to the J-domain: Nonpeptide antagonist bound $CRF_1$-J and $CRF_1$-R with similar affinity and fully blocked agonist interactions with $CRF_1$-J that activate G-protein signaling. It has also been demonstrated that nonpeptide antagonist allosterically blocks agonist binding to the $CRF_1$ receptor (*29*, *30*, *33*). Within the equilibrium model, these effects can be described by nonpeptide antagonist binding to the J-domain at a site distinct from the peptide agonist binding site, mediating negative cooperativity on the formation of $RL_{NJ}$ from $RL_N$ (Scheme 2; see Appendix). This allosteric inhibition at the J-domain is defined by the microcooperativity constant $\alpha_J$. The negative cooperativity between peptide and nonpeptide ligand binding the J-domain is likely high (see Appendix), since nonpeptide antagonist fully blocks J-domain activation by peptide agonist. According to the simulation, nonpeptide antagonist reduces peptide ligand occupancy of the J-domain within the $RL_{NJ}$ complex (Figure 8B,E, Appendix). At the R state nonpeptide antagonist only partially inhibits peptide agonist binding (*33*), a finding that can be explained by the weak contribution of the J-domain to peptide agonist binding (Figure 8A−C). At the RG state nonpeptide antagonist nearly fully blocks peptide agonist binding (*30*, *33*), a finding that can be explained by the strong contribution of the J-domain to peptide agonist binding (Figure 8D−F).

In summary, we have comprehensively evaluated the contribution of $CRF_1$ receptor domains to peptide ligand affinity. The findings of this study are consistent with the two-domain model and extend it by quantifying N- and J-domain interactions and by considering the effect of conformational modulators (G-protein and nonpeptide antagonist). Peptide agonist affinity is provided predominantly by the N-domain at the R state. The data are consistent with peptide−J-domain interaction being differentially modified by G-protein and nonpeptide antagonist, the former enhancing the interaction and the latter allosterically inhibiting it. Finally, we simulate the behavior of this model to suggest the relative occupancy of N- and J-domains by peptide ligand under a variety of conditions. These findings will be useful for further investigation of ligand interaction mechanisms for the $CRF_1$ receptor and, potentially, other secretin family GPCR's.

## APPENDIX

Peptide ligand binding to the $CRF_1$ receptor is well described by a low-resolution molecular mechanism, the two-domain hypothesis. Here an equilibrium binding model of this mechanism is presented (Scheme 1) and considered for the R and RG states of the receptor. The model is then extended to consider modulation of the receptor by nonpep-

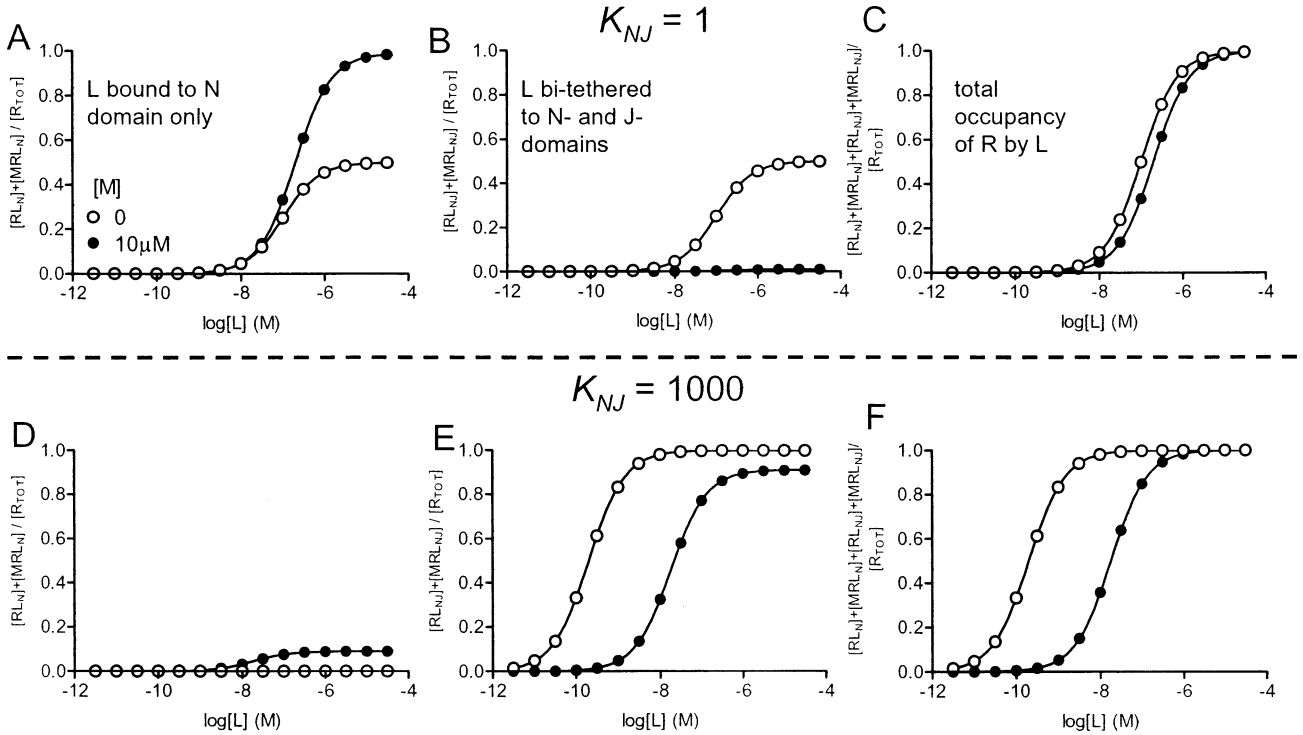


FIGURE 8: Simulation of the effect of the nonpeptide antagonist on equilibrium occupancy of N- and J-domains of the $CRF_1$ receptor by peptide ligand. Scheme 2 was used to simulate the effect of the nonpeptide antagonist (M) on peptide ligand binding to the N-domain only, $[RL_N] + [MRL_N]$ (A, D, eq 6); ligand bitethered via N- and J-domains, $[RL_{NJ}] + [MRL_{NJ}]$ (B, E, eq 7); and total ligand occupancy of the receptor, $[RL_N] + [MRL_N] + [RL_{NJ}] + [MRL_{NJ}]$ (C, F, eq 8). Binding of L was evaluated for two values of $K_{NJ}$: 1 (A−C, representing the weak peptide ligand−J-domain interaction proposed for the R state of the $CRF_1$ receptor) and 1000 (D−F, representing the strong peptide ligand−J-domain interaction proposed for the RG state of the $CRF_1$ receptor). $K_N$ was set at $5 \times 10^6$ $M^{-1}$, $K_M$ was set at $10^9$ $M^{-1}$, and the microcooperativity between L and M binding to the J-domain ($\alpha_J$) was 0.01 (representing strong negative cooperativity). Occupancy of the receptor domains by L was simulated for the absence of M (using eqs 1−3) and for the presence of a saturating concentration of M (10 $\mu$M, using eqs 6−8). $[R_{TOT}]$ was set at unity so that the *y* axis represents fractional occupancy.

Scheme 1

$$R + L \underset{}{\overset{K_N}{\rightleftharpoons}} RL_N \overset{K_{NJ}}{\rightleftharpoons} RL_{NJ}$$

tide antagonist (Scheme 2). Simulations were performed to evaluate ligand occupancy of the N-domain, the J-domain, and the whole receptor.

*Model for Equilibrium Peptide Ligand Binding to the Receptor.* Peptide ligand (L) is assumed to bind the N-domain of the receptor (R), forming $RL_N$, defined by the equilibrium association constant $K_N$ (Scheme 1). Direct peptide binding to the J-domain was extremely weak; the peptide $EC_{50}$ for $CRF_1$-J was 12000−1500000-fold higher than the $EC_{50}$ for the whole receptor in assays of cAMP accumulation (Table 4), and peptide ligands did not detectably inhibit [$^3$H]NBI 35965 binding to $CRF_1$-J (data not shown). Therefore, it is likely that ligand occupancy of the J-domain alone ($RL_J$) represents an insignificant fraction of total equilibrium occupancy of the receptor, so $RL_J$ is excluded from the model. Ligand binding to the N-domain is assumed to enormously increase the local concentration of ligand available to bind the J-domain, enabling weak interaction with the J-domain to occur. The resulting receptor−ligand complex has ligand bitethered via the two domains of the receptor ($RL_{NJ}$). The propensity of ligand to bind the J-domain once bound to the N-domain is described here by an isomerization constant, $K_{NJ}$, representing isomerization of the receptor−ligand complex from $RL_N$ to $RL_{NJ}$ and vice versa.

Equations 1−3 define equilibrium binding of L to R as a function of the total concentration of R, for the N-domain alone (eq 1), for L bitethered via both N- and J-domains (eq 2), and for total occupancy of the receptor (eq 3):

$$\frac{[RL_N]}{[R_{TOT}]} = \frac{[L]K_N}{1 + [L]K_N(1 + K_{NJ})} \quad (1)$$

$$\frac{[RL_{NJ}]}{[R_{TOT}]} = \frac{[L]K_N K_{NJ}}{1 + [L]K_N(1 + K_{NJ})} \quad (2)$$

$$\frac{[RL_N] + [RL_{NJ}]}{[R_{TOT}]} = \frac{[L]K_N(1 + K_{NJ})}{1 + [L]K_N(1 + K_{NJ})} \quad (3)$$

From eq 3 the macroaffinity contant for L binding to R ($K_L$) is given by

$$K_L = K_N(1 + K_{NJ}) \quad (4)$$

Using these equations we simulated ligand occupancy of the N-domain alone ($RL_N$), occupancy of the J-domain within the bitethered $RL_{NJ}$ complex ($RL_{NJ}$), and total occupancy of the receptor ($RL_N + RL_{NJ}$, which is also equal to total occupancy of the N-domain) (Figure 7). Ligand affinity for the N-domain was considered to be moderate ($K_N$ of $5 \times 10^6$ $M^{-1}$, 200 nM as a dissociation constant, close to the affinity of r/hCRF, oCRF, and sauvagine for $CRF_1$-N; Table 2). $K_{NJ}$ was varied to simulate the effect of varying the strength of ligand−J-domain binding. For very weak interaction with the J-domain ($K_{NJ} = 0.01$), occupancy of the J-domain ($RL_{NJ}$; Figure 7B) is much less than total oc-

cupancy of the N-domain ($RL_N + RL_{NJ}$; Figure 7C). Consequently, most of receptor occupancy is represented by ligand bound only to the N-domain ($RL_N$; Figure 7A). At saturating ligand concentrations (required to fully occupy the receptor; Figure 7C), ligand nearly fully occupies the N-domain (Figure 7C) but minimally occupies the J-domain within the $RL_{NJ}$ complex (Figure 7B). At a $K_{NJ}$ value of 1, the propensity of $RL_N$ to isomerize to $RL_{NJ}$ is equivalent to the propensity of $RL_{NJ}$ to form $RL_N$. Consequently, occupancy of $RL_N$ is equal to occupancy of $RL_{NJ}$ (Figure 7A,B), such that 50% of total receptor occupancy is represented by ligand bound only to the N-domain and 50% represented by ligand bitethered via N- and J-domains. For strong interaction with the J-domain ($K_{NJ} = 100-1000$), $RL_{NJ}$ represents almost all occupancy of the receptor (Figure 7B), with little ligand bound to only the N-domain (Figure 7A).

Using this simulation we also investigated the effect of $K_{NJ}$ on the macroaffinity of ligand for receptor ($K_L$). $K_L$ increases as the strength of ligand binding to the J-domain ($K_{NJ}$) increases (Figure 7); as evident from eq 4, macroaffinity increases by the factor $1 + K_{NJ}$ (relative to $K_N$). Consequently, for low values of $K_{NJ}$ the macroaffinity approaches $K_N$ (Figure 7). For high values of $K_{NJ}$ macroaffinity approaches the product of $K_N$ and $K_{NJ}$ (Figure 7). We investigated the value of $K_{NJ}$ for the R state. In principle, the value of $K_{NJ}$ can be determined indirectly if $K_L$ and $K_N$ are known; rearrangement of eq 4 yields

$$K_{NJ} = (K_L/K_N) - 1 \quad (5)$$

For the R state of the receptor we measured $K_L$ and $K_N$ as $1/K_i$ for $CRF_1$-R and $CRF_1$-N, respectively (Table 2). The resulting values of $K_{NJ}$ for agonist peptides are 0.1 for r/hCRF, 1.3 for oCRF, 2.5 for sauvagine, 0.9 for hUCN I, and 1.5 for rUCN I (Table 2). However, the difference between $K_L$ and $K_N$ was small, especially for r/hCRF. Consequently, the indirectly determined value of $K_{NJ}$ is highly sensitive to experimental error for each of the two affinity measurements and highly sensitive to any slight structural changes within the N-domain of $CRF_1$-N resulting from its expression in isolation. However, overall the data suggest that $K_{NJ}$ is low for peptide agonists at the R state. In consequence, for the R state we conclude that a significant fraction of total receptor occupancy by peptide agonist is represented by ligand bound to only the N-domain ($RL_N$), with the remainder represented by ligand bitethered via N- and J-domains ($RL_{NJ}$) (Figure 7).

The simulation was used to evaluate the effect of G-protein on peptide ligand interaction with the receptor. G-Protein binding likely increases the strength of peptide agonist binding to the J-domain (see Discussion). Within the context of the model, this effect is represented by an increase of $K_{NJ}$ (Figure 7). Increased $K_{NJ}$ produces a leftward shift of the receptor occupancy curve, reflecting an increase of macroaffinity resulting from R−G interaction (Figure 7C, eq 4), as observed experimentally (*33*). The value of $K_{NJ}$ for the RG state is likely high (>100), given the several hundredfold increase of macroaffinity produced by R−G interaction [Table 3 (*33*)]. Therefore, at the RG state occupancy of the N-domain alone ($RL_N$) is minimal even at saturating ligand concentrations (Figure 7A), since almost all receptor occupancy is represented by ligand bitethered via both N- and J-domains (Figure 7B). This finding suggests that relative occupancy of N- and J-domains differs between R and RG states, with greater occupancy of the N-domain alone at the R state and greater occupancy of the J-domain at the RG state.

Scheme 2

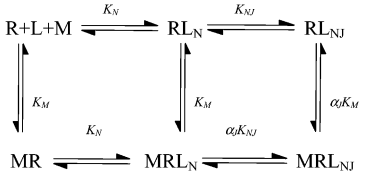


*Modulation of Peptide Ligand Binding by Nonpeptide Antagonist.* Nonpeptide antagonists have been shown to act allosterically in regulating peptide agonist binding: Nonpeptide antagonist binding is reduced by amino acid changes that do not affect binding of peptide agonist (*29*), and binding data are consistent with allosteric interaction between peptide and nonpeptide ligand binding (*30*, *33*). This mechanism is represented in Scheme 2. Peptide ligand (L) binds N- and J-domains, defined by $K_N$ and $K_{NJ}$, respectively (Scheme 1). Nonpeptide antagonist (M) binds only to the J-domain, defined by the equilibrium association constant $K_M$. The microcooperativity constant $\alpha_J$ defines the effect of M binding on L binding to the J-domain and vice versa. We assume M binding does not affect L binding to the N-domain, consistent with the findings of this study.

Equations 6−8 define equilibrium binding of L to R in the presence of M for the N-domain alone (eq 6), for L bitethered via both N- and J-domains (eq 7), and for total occupancy of the receptor (eq 8):

$$\frac{[RL_N] + [MRL_N]}{[R_{TOT}]} = \frac{[L]K_N(1 + [M]K_M)}{1 + [L]K_N(1 + K_{NJ}) + [L][M]K_NK_M(1 + \alpha_JK_{NJ}) + [M]K_M} \quad (6)$$

$$\frac{[RL_{NJ}] + [MRL_{NJ}]}{[R_{TOT}]} = \frac{[L]K_NK_{NJ}(1 + [M]\alpha_JK_M)}{1 + [L]K_N(1 + K_{NJ}) + [L][M]K_NK_M(1 + \alpha_JK_{NJ}) + [M]K_M} \quad (7)$$

$$\frac{[RL_N] + [MRL_N] + [RL_{NJ}] + [MRL_{NJ}]}{[R_{TOT}]} = \frac{[L]K_N(1 + K_{NJ}) + [L][M]K_NK_M(1 + \alpha_JK_{NJ})}{1 + [L]K_N(1 + K_{NJ}) + [L][M]K_NK_M(1 + \alpha_JK_{NJ}) + [M]K_M} \quad (8)$$

We simulated the behavior of Scheme 2 using the following parameter estimates: $K_N$ was estimated as described above ($5 \times 10^6\ M^{-1}$). Two values of $K_{NJ}$ were used: 1, representing weak peptide interaction with the J-domain assumed for the R state of the receptor, and 1000, representing strong peptide interaction with the J-domain assumed for the RG state (see above). $K_M$ was set at $1 \times 10^9\ M^{-1}$ (Table 1), and [M] was fixed at a saturating concentration

($1 \times 10^{-5}$ M). In defining $\alpha_J$, it was assumed that negative cooperativity at the J-domain was strong ($\alpha_J = 0.01$) for two reasons: (1) Nonpeptide antagonist nearly fully blocks [$^{125}$I]-sauvagine binding to the RG state (a strong J-domain peptide binding interaction). (2) M fully blocks L-mediated signaling via $CRF_1$-J.

Using eqs 6−8 and the values above, we simulated L occupancy of the N-domain only ($RL_N + MRL_N$), L occupancy of the J-domain within the bitethered RL complex ($RL_{NJ} + MRL_{NJ}$), and total occupancy of the receptor by L (Figure 8). For a $K_{NJ}$ value of unity (assumed to represent the R state) it is evident that M nearly completely inhibits L binding to the J-domain (Figure 8B), even at saturating concentrations of L. Since J-domain binding is displaced from within the $RL_{NJ}$ complex, essentially all peptide ligand occupancy of the receptor is represented by ligand bound to only the N-domain (Figure 8A). Total receptor occupancy by L is only moderately affected by saturating concentrations of M at the R state (Figure 8C), as observed experimentally (*33*). This is because the interaction of L inhibited by M (that with the J-domain) contributes only a small amount to the macroaffinity of L at the R state.

For a $K_{NJ}$ value of 1000 (assumed to represent the RG state) a saturating concentration of M produces a large rightward shift of the ligand occupancy curve for the J-domain within the $RL_{NJ}$ complex (Figure 8E). At saturating concentrations of L occupancy of the J-domain is only slightly reduced by M (Figure 8E). Therefore, in contrast to the R state, M fails to fully displace L binding to the J-domain in this simulation. This is because L's interaction with the J-domain is strong ($K_{NJ} = 1000$). Consequently, though negative cooperativity is high ($\alpha_J = 0.01$), L interaction with the J-domain, defined by $\alpha_J K_{NJ}$, is moderate ($\alpha_J K_{NJ} = 10$). Saturating concentrations of M slightly increase the occupancy of the N-domain alone (Figure 8D), resulting from the displacement of L binding to the J-domain. The occupancy curve for total receptor occupancy by L is shifted rightward to a large extent by M (Figure 8F), because the J-domain interaction of L, inhibited by M, contributes considerably to the macroaffinity of L. As a result, binding of low concentrations of L (100 pM) is blocked nearly completely by M [as observed experimentally for nonpeptide antagonist-mediated inhibition of [$^{125}$I]sauvagine and [$^{125}$I]-CRF binding to the RG state (*30*, *33*)]. However, saturating concentrations of M do not prevent L occupancy of the receptor; M does not affect the moderate microaffinity of L for the N-domain ($K_N = 5 \times 10^6$ $M^{-1}$), and as described above binding to the J-domain is strongly reduced but remains of moderate strength ($K_{NJ} = 10$). Consequently, receptor binding of L can be detected at higher concentrations of L [e.g., 1 nM, as observed experimentally for NBI 35965-mediated inhibition of [$^{125}$I]sauvagine binding to the RG state (*33*)].

It is important to note that while this simulation above accounts for the current experimental observations, other parameter estimates can also account for the data. Notably, we have determined previously that the macrocooperativity constant between L and M binding ($\alpha$) is less at the RG state than at the R state (representing greater negative cooperativity). The macrocooperativity $\alpha$ is dependent on the microcooperativity on the J-domain ($\alpha_J$) and the strength of ligand binding to the J-domain ($K_{NJ}$), shown as follows.

The equation defining the effect of M on the macroaffinity of L is given by (*33*, *51*)

$$\frac{[RL] + [MRL]}{[R_{TOT}]} = \frac{[L]K_L(1 + \alpha[M]K_M)}{1 + [L]K_L(1 + \alpha[M]K_M) + [M]K_M} \quad (9)$$

By comparing eq 9 with the equation defining the effect of M on the microaffinity of L (eq 8), it is evident that

$$[L]K_L(1 + \alpha[M]K_M) = [L]K_N(1 + K_{NJ}) + [L][M]K_NK_M(1 + \alpha_J K_{NJ})$$

By substituting $K_N(1 + K_{NJ})$ for $K_L$ and rearranging, we obtain

$$\alpha = \frac{1 + \alpha_J K_{NJ}}{1 + K_{NJ}} \quad (10)$$

In this simulation the decreased value of $\alpha$ at the RG state compared with the R state is assumed to be solely due to an increase of $K_{NJ}$. As a result the current simulation is the simplest that can account for the data. However, the current data do not exclude the possibility that the microcooperativity ($\alpha_J$) differs between R and RG states.

## ACKNOWLEDGMENT

We gratefully acknowledge Xin-Jin Liu for synthesis of [$^{125}$I]astressin and Anil Pahuja for technical assistance.

## REFERENCES

1. Chang, C. P., Pearse, R. V., II, O'Connell, S., and Rosenfeld, M. G. (1993) Identification of a seven transmembrane helix receptor for corticotropin-releasing factor and sauvagine in mammalian brain, *Neuron 11*, 1187−1195.
2. Chen, R., Lewis, K. A., Perrin, M. H., and Vale, W. W. (1993) Expression cloning of a human corticotropin-releasing-factor receptor, *Proc. Natl. Acad. Sci. U.S.A. 90*, 8967−8971.
3. Vita, N., Laurent, P., Lefort, S., Chalon, P., Lelias, J. M., Kaghad, M., Le Fur, G., Caput, D., and Ferrara, P. (1993) Primary structure and functional expression of mouse pituitary and human brain corticotrophin releasing factor receptors, *FEBS Lett. 335*, 1−5.
4. Dautzenberg, F. M., and Hauger, R. L. (2002) The CRF peptide family and their receptors: yet more partners discovered, *Trends Pharmacol. Sci. 23*, 71−77.
5. Vale, W., Spiess, J., Rivier, C., and Rivier, J. (1981) Characterization of a 41-residue ovine hypothalamic peptide that stimulates secretion of corticotropin and beta-endorphin, *Science 213*, 1394−1397.
6. Vaughan, J., Donaldson, C., Bittencourt, J., Perrin, M. H., Lewis, K., Sutton, S., Chan, R., Turnbull, A. V., Lovejoy, D., Rivier, C., Rivier, J., Sawchenko, P. E., and Vale, W. W. (1995) Urocortin, a mammalian neuropeptide related to fish urotensin I and to corticotropin-releasing factor, *Nature 378*, 287−292.
7. Moreau, J. L., Kilpatrick, G., and Jenck, F. (1997) Urocortin, a novel neuropeptide with anxiogenic-like properties, *Neuroreport 8*, 1697−1701.
8. Vetter, D. E., Li, C., Zhao, L., Contarino, A., Liberman, M. C., Smith, G. W., Marchuk, Y., Koob, G. F., Heinemann, S. F., Vale, W., and Lee, K. F. (2002) Urocortin-deficient mice show hearing impairment and increased anxiety-like behavior, *Nat. Genet. 31*, 363−369.
9. Montecucchi, P. C., and Henschen, A. (1981) Amino acid composition and sequence analysis of sauvagine, a new active peptide from the skin of *Phyllomedusa Sauvagei*, *Int. J. Pept. Protein Res. 18*, 113−120.
10. Holsboer, F. (1999) The rationale for corticotropin-releasing hormone receptor (CRH-R) antagonists to treat depression and anxiety, *J. Psychiatr. Res. 33*, 181−214.

11. Grigoriadis, D. E., Haddach, M., Ling, N., and Saunders, J. (2001) The CRF receptor: Structure, function and potential for therapeutic intervention, *Curr. Med. Chem.: Cent. Nerv. Syst. Agents 1*, 63−97.
12. Gilligan, P. J., Robertson, D. W., and Zaczek, R. (2000) Corticotropin releasing factor (CRF) receptor modulators: progress and opportunities for new therapeutic agents, *J. Med. Chem. 43*, 1641−1660.
13. Perrin, M. H., and Vale, W. W. (1999) *Ann. N.Y. Acad. Sci.*, 312−328.
14. Assil, I. Q., Qi, L. J., Arai, M., Shomali, M., and Abou-Samra, A. B. (2001) Juxtamembrane region of the amino terminus of the corticotropin releasing factor receptor type 1 is important for ligand interaction, *Biochemistry 40*, 1187−1195.
15. Hofmann, B. A., Sydow, S., Jahn, O., van Werven, L., Liepold, T., Eckart, K., and Spiess, J. (2001) Functional and protein chemical characterization of the N-terminal domain of the rat corticotropin-releasing factor receptor 1, *Protein Sci. 10*, 2050−2062.
16. Perrin, M. H., Fischer, W. H., Kunitake, K. S., Craig, A. G., Koerber, S. C., Cervini, L. A., Rivier, J. E., Groppe, J. C., Greenwald, J., Moller Nielsen, S., and Vale, W. W. (2001) Expression, purification, and characterization of a soluble form of the first extracellular domain of the human type 1 corticotropin releasing factor receptor, *J. Biol. Chem. 276*, 31528−31534.
17. Nielsen, S. M., Nielsen, L. Z., Hjorth, S. A., Perrin, M. H., and Vale, W. W. (2000) Constitutive activation of tethered-peptide/corticotropin-releasing factor receptor chimeras, *Proc. Natl. Acad. Sci. U.S.A. 97*, 10277−10281.
18. Perrin, M. H., Sutton, S., Bain, D. L., Berggren, W. T., and Vale, W. W. (1998) The first extracellular domain of corticotropin releasing factor-R1 contains major binding determinants for urocortin and astressin, *Endocrinology 139*, 566−570.
19. Rivier, J., Rivier, C., and Vale, W. (1984) Synthetic competitive antagonists of corticotropin-releasing factor: effect on ACTH secretion in the rat, *Science 224*, 889−891.
20. Beyermann, M., Rothemund, S., Heinrich, N., Fechner, K., Furkert, J., Dathe, M., Winter, R., Krause, E., and Bienert, M. (2000) A role for a helical connector between two receptor binding sites of a long-chain peptide hormone, *J. Biol. Chem. 275*, 5702−5709.
21. Wille, S., Sydow, S., Palchaudhuri, M. R., Spiess, J., and Dautzenberg, F. M. (1999) Identification of amino acids in the N-terminal domain of corticotropin-releasing factor receptor 1 that are important determinants of high-affinity ligand binding, *J. Neurochem. 72*, 388−395.
22. Dautzenberg, F. M., Kilpatrick, G. J., Wille, S., and Hauger, R. L. (1999) The ligand-selective domains of corticotropin-releasing factor type 1 and type 2 receptor reside in different extracellular domains: generation of chimeric receptors with a novel ligand-selective profile, *J. Neurochem. 73*, 821−829.
23. Dautzenberg, F. M., Wille, S., Lohmann, R., and Spiess, J. (1998) Mapping of the ligand-selective domain of the *Xenopus laevis* corticotropin-releasing factor receptor 1: implications for the ligand-binding site, *Proc. Natl. Acad. Sci. U.S.A. 95*, 4941−4946.
24. Liaw, C. W., Grigoriadis, D. E., Lovenberg, T. W., De Souza, E. B., and Maki, R. A. (1997) Localization of ligand-binding domains of human corticotropin-releasing factor receptor: a chimeric receptor approach, *Mol. Endocrinol. 11*, 980−985.
25. Dautzenberg, F. M., Higelin, J., Brauns, O., Butscha, B., and Hauger, R. L. (2002) Five amino acids of the *Xenopus laevis* CRF (corticotropin-releasing factor) type 2 receptor mediate differential binding of CRF ligands in comparison with its human counterpart, *Mol. Pharmacol. 61*, 1132−1139.
26. Sydow, S., Flaccus, A., Fischer, A., and Spiess, J. (1999) The role of the fourth extracellular domain of the rat corticotropin-releasing factor receptor type 1 in ligand binding, *Eur. J. Biochem. 259*, 55−62.
27. Sydow, S., Radulovic, J., Dautzenberg, F. M., and Spiess, J. (1997) Structure−function relationship of different domains of the rat corticotropin-releasing factor receptor, *Mol. Brain Res. 52*, 182−193.
28. Assil-Kishawi, I., and Abou-Samra, A. B. (2002) Sauvagine cross-links to the second extracellular loop of the corticotropin-releasing factor type 1 receptor, *J. Biol. Chem. 277*, 32558−32561.
29. Liaw, C. W., Grigoriadis, D. E., Lorang, M. T., De Souza, E. B., and Maki, R. A. (1997) Localization of agonist- and antagonist-binding domains of human corticotropin-releasing factor receptors, *Mol. Endocrinol. 11*, 2048−2053.
30. Zhang, G., Huang, N., Li, Y. W., Qi, X., Marshall, A. P., Yan, X. X., Hill, G., Rominger, C., Prakash, S. R., Bakthavatchalam, R., Rominger, D. H., Gilligan, P. J., and Zaczek, R. (2003) Pharmacological characterization of a novel nonpeptide antagonist radioligand, (±)-N-[2-methyl-4-methoxyphenyl]-1-(1-(methoxymethyl) propyl)-6-methyl-1H-1,2,3-triazolo[4,5-c]pyridin-4-amine ([3H]SN003) for corticotropin-releasing factor1 receptors, *J. Pharmacol. Exp. Ther. 305*, 57−69.
31. Perrin, M. H., Haas, Y., Rivier, J. E., and Vale, W. W. (1986) Corticotropin-releasing factor binding to the anterior pituitary receptor is modulated by divalent cations and guanyl nucleotides, *Endocrinology 118*, 1171−1179.
32. Hoare, S. R. J., Sullivan, S. K., Pahuja, A., Ling, N., Crowe, P. D., and Grigoriadis, D. E. (2003) Conformational states of the corticotropin releasing factor 1 (CRF1) receptor: detection, and pharmacological evaluation by peptide ligands, *Peptides 24*, 1881−1897.
33. Hoare, S. R. J., Sullivan, S. K., Ling, N., Crowe, P. D., and Grigoriadis, D. E. (2003) Mechanism of Corticotropin-Releasing Factor Type I Receptor Regulation by Nonpeptide Antagonists, *Mol. Pharmacol. 63*, 751−765.
34. Hsu, S. Y., and Hsueh, A. J. (2001) Human stresscopin and stresscopin-related peptide are selective ligands for the type 2 corticotropin-releasing hormone receptor, *Nat. Med. 7*, 605−611.
35. Reyes, T. M., Lewis, K., Perrin, M. H., Kunitake, K. S., Vaughan, J., Arias, C. A., Hogenesch, J. B., Gulyas, J., Rivier, J., Vale, W. W., and Sawchenko, P. E. (2001) Urocortin II: A member of the corticotropin-releasing factor (CRF) neuropeptide family that is selectively bound by type 2 CRF receptors, *Proc. Natl. Acad. Sci. U.S.A. 98*, 2843−2848.
36. Lewis, K., Li, C., Perrin, M. H., Blount, A., Kunitake, K., Donaldson, C., Vaughan, J., Reyes, T. M., Gulyas, J., Fischer, W., Bilezikjian, L., Rivier, J., Sawchenko, P. E., and Vale, W. W. (2001) Identification of urocortin III, an additional member of the corticotropin-releasing factor (CRF) family with high affinity for the CRF2 receptor, *Proc. Natl. Acad. Sci. U.S.A. 98*, 7570−5.
37. Miranda, A., Koerber, S. C., Gulyas, J., Lahrichi, S. L., Craig, A. G., Corrigan, A., Hagler, A., Rivier, C., Vale, W., and Rivier, J. (1994) Conformationally restricted competitive antagonists of human/rat corticotropin-releasing factor, *J. Med. Chem. 37*, 1450−1459.
38. Rivier, J., Gulyas, J., Kirby, D., Low, W., Perrin, M. H., Kunitake, K., DiGruccio, M., Vaughan, J., Reubi, J. C., Waser, B., Koerber, S. C., Martinez, V., Wang, L., Tache, Y., and Vale, W. (2002) Potent and Long-Acting Corticotropin Releasing Factor (CRF) Receptor 2 Selective Peptide Competitive Antagonists, *J. Med. Chem. 45*, 4737−4747.
39. Ruhmann, A., Bonk, I., Lin, C. R., Rosenfeld, M. G., and Spiess, J. (1998) Structural requirements for peptidic antagonists of the corticotropin-releasing factor receptor (CRFR): development of CRFR2beta-selective antisauvagine-30, *Proc. Natl. Acad. Sci. U.S.A. 95*, 15264−15269.
40. Mathews, L. S., and Vale, W. W. (1991) Expression cloning of an activin receptor, a predicted transmembrane serine kinase, *Cell 65*, 973−982.
41. Cheng, Y., and Prusoff, W. H. (1973) Relationship between the inhibition constant (K1) and the concentration of inhibitor which causes 50% inhibition (I50) of an enzymatic reaction, *Biochem. Pharmacol. 22*, 3099−3108.
42. Webster, E. L., Lewis, D. B., Torpy, D. J., Zachman, E. K., Rice, K. C., and Chrousos, G. P. (1996) In vivo and in vitro characterization of antalarmin, a nonpeptide corticotropin-releasing hormone (CRH) receptor antagonist: suppression of pituitary ACTH release and peripheral inflammation, *Endocrinology 137*, 5747−5750.
43. Chen, C., Dagnino, R., Jr., De Souza, E. B., Grigoriadis, D. E., Huang, C. Q., Kim, K. I., Liu, Z., Moran, T., Webb, T. R., Whitten, J. P., Xie, Y. F., and McCarthy, J. R. (1996) Design and synthesis of a series of non-peptide high-affinity human corticotropin-releasing factor1 receptor antagonists, *J. Med. Chem. 39*, 4358−4360.
44. He, L., Gilligan, P. J., Zaczek, R., Fitzgerald, L. W., McElroy, J., Shen, H. S., Saye, J. A., Kalin, N. H., Shelton, S., Christ, D.,

Trainor, G., and Hartig, P. (2000) 4-(1,3-Dimethoxyprop-2-ylamino)-2,7-dimethyl-8-(2,4-dichlorophenyl)pyrazolo[1,5-a]-1,3,5-triazine: a potent, orally bioavailable CRF(1) receptor antagonist, *J. Med. Chem. 43*, 449−456.

45. Luck, M. D., Carter, P. H., and Gardella, T. J. (1999) The (1−14) fragment of parathyroid hormone (PTH) activates intact and amino-terminally truncated PTH-1 receptors, *Mol. Endocrinol. 13*, 670−680.
46. Hoare, S. R. J., Gardella, T. J., and Usdin, T. B. (2001) Evaluating the signal transduction mechanism of the parathyroid hormone 1 receptor. Effect of receptor-G-protein interaction on the ligand binding mechanism and receptor conformation, *J. Biol. Chem. 276*, 7741−7753.
47. Shimizu, N., Guo, J., and Gardella, T. J. (2001) Parathyroid hormone (PTH)-(1−14) and -(1−11) analogs conformationally constrained by alpha-aminoisobutyric acid mediate full agonist responses via the juxtamembrane region of the PTH-1 receptor, *J. Biol. Chem. 276*, 49003−49012.
48. Assil, I. Q., and Abou-Samra, A. B. (2001) N-glycosylation of CRF receptor type 1 is important for its ligand-specific interaction, *Am. J. Physiol. Endocrinol. Metab. 281*, E1015−E1021.
49. Perrin, M. H., DiGruccio, M. R., Koerber, S. C., Rivier, J. E., Kunitake, K. S., Bain, D. L., Fischer, W. H., and Vale, W. W. (2003) A soluble form of the first extracellular domain of mouse type 2beta corticotropin-releasing factor receptor reveals differential ligand specificity, *J. Biol. Chem. 278*, 15595−15600.
50. Al-Sabah, S., and Donnelly, D. (2003) A model for receptor-peptide binding at the glucagon-like peptide-1 (GLP-1) receptor through the analysis of truncated ligands and receptors, *Br. J. Pharmacol. 140*, 339−346.
51. Lazareno, S., and Birdsall, N. J. (1995) Detection, quantitation, and verification of allosteric interactions of agents with labeled and unlabeled ligands at G protein-coupled receptors: interactions of strychnine and acetylcholine at muscarinic receptors, *Mol. Pharmacol. 48*, 362−378.

BI036110A